European Polymer Journal 209 (2024) 112864

Contents lists available at ScienceDirect

European Polymer Journal

journal homepage: www.elsevier.com/locate/europolj

3D-bioprinting of self-healing hydrogels

Jennika Karvinen *, Minna Kellomäki

Biomaterials and Tissue Engineering Group, Faculty of Medicine and Health Technology and BioMediTech Institute, Tampere University, Tampere, Finland

ARTICLE INFO

Keywords:
3D-bioprinting
Hydrogel
Self-healing

ABSTRACT

Self-healing hydrogels are the most promising hydrogel-ink materials, especially for extrusion-based 3D-bioprinting, because, unlike traditional hydrogels, the bonds as well as their initial structure, properties and functionality can be recovered after extrusion, which together with shear-thinning property enables safe printing for cells, but also shape stability of the construct after printing. In addition to tunable viscoelastic properties given by these inks, they can also respond to cell forces by rearranging the network, while maintaining bulk physiological properties. Currently, mainly extrusion-based bioprinting has been used for these types of dynamic inks. Some basic 3D structures, such as letters, grids and patterns, have been printed with high shape fidelity and high cell viability using traditional 3D-bioprinting. More complex spiral, pyramidal, or vascular tree structures have also been printed using so-called gel-in-gel printing technique, and even some overhang geometries without the need for additional support bath. The current limitation of self-healing hydrogel inks has been their poor mechanical stability, which has been improved, for example, using additional crosslinking. However, the opposing characteristics of self-healing hydrogels, like toughness and fast self-healability, remain a challenge. Therefore, more studies are needed in the future to improve the self-healing hydrogel inks. This review collects some of the most relevant studies related to self-healing 3D-bioprintable hydrogels. It also discusses the importance of self-healing and shear-thinning properties for bioinks and bioprinted constructs, the effects of self-healing hydrogel bioinks and bioprinting on cells (and vice versa), as well as the current status and future prospects of self-healing hydrogel bioinks.

1. Introduction

Bioprinting has become an established technique to create constructs with natural tissue-like three-dimensional (3D) structures for use in tissue engineering (TE) and drug development. In bioprinting, bioink refers to specialized living cells, and hydrogel-based biomaterial which provides structural and mechanical support to cells [1–3]. Despite similarities to injectable hydrogels, the requirements for ideal 3D-bioprintable hydrogel inks are more strict. For example, an ideal hydrogel bioink for extrusion-based bioprinting (EBB) should be printable, extrudable, readily manipulated by the printer, contain sterile and endotoxin-free starting materials, and have tunable physical, chemical, functional, material, and biological properties. In addition, suitable viscosity and rheological properties are needed, as well as stability during the printing procedure. In terms of cells, their homogeneous distribution should be enabled, as well as considering manufacturing impact on their viability (i.e., chemical cytotoxicity, pressure-induced apoptotic effect, etc.) [3–13]. The formed 3D-bioprinted tissue construct, on the other hand, should be functionally biomimicking (e.g., complex neural structures, internal vasculature, and circulation), ensure shape stability and self-supporting structure, be flexible, tolerate dynamic mechanical loads, have minor or no swelling, and have a structure that promotes nutrient and waste transportation, and cell (in) growth, proliferation and cell signaling [3–13].

Hydrogels are suitable ink materials for 3D-bioprinting due to their similarity to extracellular matrix (ECM) [14]. They can facilitate cell adhesion and migration, as well as matrix remodeling in 3D environment, which is needed for the normal development of functional tissues [7]. However, due to their covalent bonds, traditional hydrogels are poorly resistant to mechanical forces exerted by the environment [15]. When the irreversible bonds are broken, the structure breaks down, and the hydrogel cannot guarantee a stable growth environment for the cells. The broken structure can also expose the repairing tissue to infections [16]. This is not a problem for so-called self-healing hydrogels, as they are able to modify their bonds according to the environment. Unlike traditional hydrogels, self-healing hydrogels, inspired by the healing

* Corresponding author.
E-mail address: jennika.karvinen@tuni.fi (J. Karvinen).

https://doi.org/10.1016/j.eurpolymj.2024.112864
Received 3 July 2023; Received in revised form 15 February 2024; Accepted 17 February 2024
Available online 23 February 2024

ability of the body *in vivo* (e.g., wound healing), are able to recover the broken bonds of the network (in seconds to hours) after damage, i.e., their initial structure, properties, and functionality can be restored from micro- to macroscale, ideally rapidly and repeatedly [17,16,14]. Therefore, they can have extended lifetimes and can, for example, tolerate the structural deformation in the body better, and thus also be cost-effective [14,18]. In addition to durability, they can also have increased reliability as well as safety as they avoid the crack accumulation-caused failures [17]. Self-healing hydrogels are also able to adapt to the needs of the cells growing inside them. In this way, the growth conditions remain more stable than in traditional hydrogels [15].

The self-healing ability is facilitated by the bonding type (Fig. 1) of these hydrogels, i.e., they can be formed by dynamic covalent (e.g. acylhydrazone bonds, imine bonds, Diels–Alder reactions, disulfide bonds, and boronate ester bonds) or non-covalent supramolecular (e.g., hydrogen bonds, hydrophobic interactions, ionic interactions, electrostatics, host–guest interactions, metal–ligand coordination complexes and peptide self-assembling) interactions [19]. The recovery time and percentage, as well as mechanical and physical properties of hydrogels will range depending on the interaction type [10]. Dynamic covalent interactions are considered stronger (and more stable) than dynamic physical supramolecular interactions [10]. For example, in terms of storage-modulus strength, a decreasing strength (from MPa to Pa) covalent bonding > ionic bonding > hydrogen bonding ≈ hydrophobic bonding > supramolecular interactions has been found [17]. Therefore, the former are considered more sensitive to mechanical shearing, but on the other hand, faster in terms of recovery compared with dynamic covalent interactions (more stable materials) [10,5]. This means that with increasing healing efficiency the healing time is faster [10]. The healing can happen either autonomously, i.e., the damage is healed intrinsically and automatically through a physical connection in as-prepared materials without any external stimuli, or with the help of some external stimulus, such as temperature, pH, or ultraviolet (UV) light [17,20].

The limitation of current self-healing hydrogels, however, has been their poor mechanical stability if only physical crosslinks are used, which could, however, be solved by stabilizing the gel with additional crosslinks (e.g., hybrid, interpenetrating networks, or nanocomposites) [17,21–23]. However, the opposing characteristics of self-healing hydrogels, like toughness and fast self-healability, remain a challenge [24,25]. Current self-healing hydrogels are also usually nonconductive, and, for example, have lower fracture energies compared with muscle tissues, skin or cartilage which limits their use in these electrically active elastic tissues [24]. Further, the use of crosslinking chemicals that are potentially toxic, or preparation techniques that are complicated, can limit larger scale production of self-healing hydrogels [18].

The selection of suitable printing technique is important because it affects the selection of bioink and their printability, as well as the properties of the printed construct [8]. Four printing techniques, i.e., extrusion-based (EBB), inkjet-based (a type of droplet-based (DBB)), laser assisted (LBB), and stereolithography are widely used for bioprinting [1,3,4,8–10,13,26–33]. For dynamic inks, mainly EBB is used, but there are also some inkjet- and stereolithography-based studies as well [17,34,35]. EBB is usually used if considerable mechanical strength is required, by using so-called support materials, i.e., extruding the gel

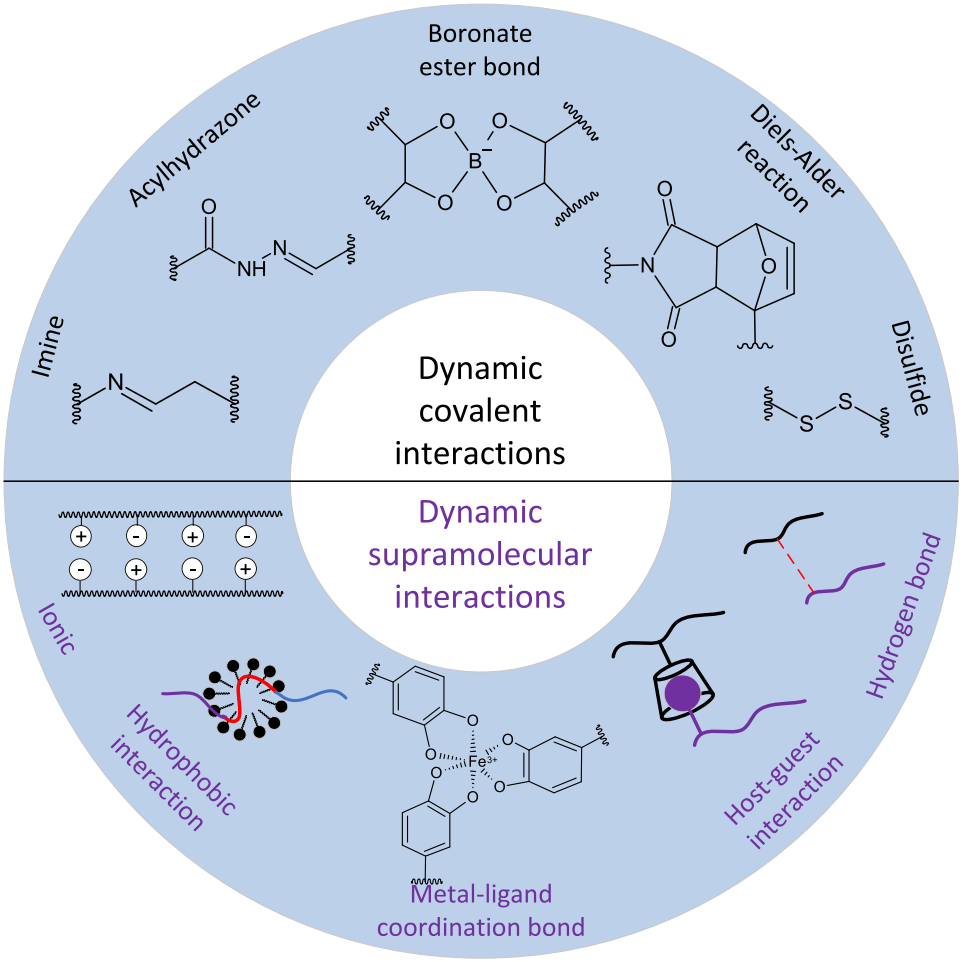

Fig. 1. Dynamic covalent and supramolecular interaction types.

into a secondary support gel [13,3,36]. When using high viscosity bioinks, EBB also requires shear-thinning bioink, that together with self-healing properties enable withstanding of high shear forces and rapid recovery after printing that are needed for protection and better viability of cells [9,37,28].

The purpose of this review article is to familiarize with the relevant research in the field, and possible challenges and future prospects related to self-healing 3D-bioprintable hydrogels. The importance of self-healing and shear-thinning properties for bioinks and bioprinted tissue constructs, and their effects on cells are also discussed.

2. The importance of hydrogels' shear-thinning and self-healing properties for bioink, bioprinting, and cells

There are many design aspects that need to be considered when designing hydrogel-based bioinks. For example, for EBB, which is the most common printing technique for dynamic inks, there are many material properties, including shear-thinning and self-healing properties, that affect the bioink's printability [3]. In the case of EBB, printability refers to suitable extrudability, filament formation, and shape fidelity [38]. Balancing yield stress, shear-thinning and recoverability is crucial for achieving high shape fidelity [37,28,3]. It is also important to understand the rheological properties of bioink in all of the printing stages. In the extrusion stage, bioink's viscosity, yield stress, and shear-thinning properties matter. In the recovery stage, it is important to know bioink's shear recovery, whereas in the self-supporting stage, yield stress becomes important again [39]. In this section the impact of hydrogels' shear-thinning and self-healing properties on bioink behavior and bioprinting, as well as the impact of bioink's properties and bioprinting on cells and vice versa are described more deeply.

2.1. Impact of hydrogels' shear-thinning and self-healing properties for bioink behavior and bioprinting

Shear-thinning materials have shear-rate-dependent behavior, meaning that as the shear rate increases the viscosity decreases, which makes shear-thinning hydrogels good candidates for bioinks [4,28,23,3]. Shear-thinning property is important for printability, extrudability, and injectability because deposition of bioink, i.e., its smooth flow through the nozzle, is facilitated when viscosity decreases due to applied pressure in the nozzle. This is crucial for enhanced resolution and high shape fidelity [7,28,40]. Viscosity decreases due to breaking of the physical crosslinks and aligning of chains, which decreases the extend of entanglements [41]. When shear stress is removed, bioink's viscosity increases again [28]. If material does not shear thin, it may clog the nozzle [42]. In addition, since shear-thinning materials are not time-dependent, they can be considered ideal bioinks, i.e., the viscosity is constant over time, unlike with thixotropic materials whose viscosity decreases with time and can lead to inhomogeneous dispensing and uneven distribution of cells or particles [4,37,43,3].

The problem with some shear-thinning hydrogels is their prolonged recovery time after extrusion (due to enabled long-range interactions between the specific binding molecules on macromers, or nonspecific interactions between the macromers), which can lead to low shape fidelity [44,23]. However, by combining shear-thinning and self-healing properties in one bioink, this challenge can be overcome, i.e., the bioink behaves as a liquid during extrusion and rapidly solidifies (structural recovery) after deposition [14,23].

Self-healing hydrogels can be formed through non-covalent supramolecular (physical) and/or dynamic chemical crosslinking. Supramolecular chemistry is suitable for bioprinting since these hydrogels are sensitive to stimuli, such as mechanical or thermal stimulus, which enables the dynamic breaking of interactions when applying the stimulus and reforming when the stimulus is removed [45]. Each type of non-covalent interaction has different binding strength which enables different mechanical properties for the bioink [46]. However, the lack of good mechanical properties of these non-covalent supramolecular hydrogel-based bioinks can cause stability issues and difficulties in handling of the construct [7]. Thus, basic chemical crosslinking can be used to stabilize the construct after printing, for example, a hydrogel with dynamic supramolecular bonding, having shear-thinning and supporting properties can be stabilized with covalent crosslinking (UV induced), enabling direct printing on the ink into self-healable structures, which would further have potential in bioprinting of multi-material complex constructs [47]. Due to more unstable nature of physically crosslinked hydrogels, they are better suited as fugitive sacrificial templates having temporal stability (e.g., bioprinted vascular structures), whereas covalently crosslinked hydrogels with long-term stability are suitable for constructive bioprinting [48,49,3]. Since different bonds have different dissociation energies, those can be approximately translated to pressure that is required to extrude them [45]. In the case of dynamic covalent bonds, the dissociation energy is intermediate, and lower than with traditional covalent bonds, which enables the reversibility under certain conditions [45].

The interactions between the molecules influence the recovery time and transition process [7]. Compared with injectable systems, the solidification conditions of printing systems are more strict because the acceptable gelation time is shorter and the nozzle diameters are smaller for printing [4,3]. Fast structure recovery after extrusion can improve shape fidelity and enable high resolution, i.e., construct sagging is reduced and there is more room for post-crosslinking [39,42,3]. The recommended recovery time for bioprinting is relatively quick, i.e., 5–10 s (>85% of storage modulus (G')) [42,3].

There are also other 3D-bioprinting challenges of traditional hydrogel-based bioinks that hydrogels with shear-thinning and self-healing properties can overcome. It is known that the bioink must withstand external forces, such as the weight of stacking layers, after extrusion and recovery in order to prevent poor shape fidelity and enable self-supporting tissue construct [42,3]. After printing, extruded filaments with sufficient mechanical strength for maintaining the shape and supporting the next printed layers can be achieved by using highly shear-thinning hydrogels [41,3]. However, the challenge is to create hydrogels with shear-thinning properties that are matched to the shearing forces of the target tissue so that the hydrogel-based tissue construct could handle the dynamic movements of the target tissue and would not disintegrate [24].

With many traditional hydrogel-based bioinks, fast mechanical stabilization after extrusion is not allowed [23]. Traditional hydrogels are also unable to mimic the biological tissue's hierarchical complexity because the microenvironments are uniform and static. They also have limited structural complexity, large equilibrium volume swelling, and brittle nature [10]. Hydrogel's reversible interactions not only provide desirable mechanical properties (mechanical strength and elasticity) but also enhance the shear-thinning which further improves the printability [50]. Thus, by using self-healing hydrogels, there is no need to consider the control of gelling process for mechanical stabilization purposes [44].

The 3D-(bio) printing of large-sized and more complex constructs using soft hydrogel-based inks is difficult since the deposited structure easily collapses. This could be overcome by using so-called gel-in-gel printing or modular printing [44], both of which self-healing hydrogels are good candidates for, as will be shown later in Section 3. In addition, by using shear-thinning self-healing hydrogels, the improvement of interlayer adhesions between weld lines is possible, as well as printing those more complex objects [10]. These hydrogels also enable the increasing of printing speed (which is very desired) without object property deterioration [10].

Wide characterization of pre- and post-printing properties of inks helps to improve the final bioprinted constructs. For example, Karvinen et al. [3] have collected different pre- and post-printing characterization methods for (bio) inks and (bio) printed constructs, including how to characterize shear-thinning behavior. In another paper, Karvinen et al. [51] have shown how the self-healing property of hydrogels can be fully

characterized, starting from determining the presence of reversible interactions to determining self-healability or healing efficiency of hydrogels.

2.2. Impact of bioink's properties and bioprinting on cells and vice versa

Morgan et al. [52] have presented the three roles for ideal bioink: (1) to maintain cell viability by protecting cells from shear stress, allowing biomolecule and nutrient diffusion, and offering adhesion sites (cells can interact with the matrix); (2) to be bioprintable by being mechanically compatible with the printing technique; and 3) to direct cell behavior by offering mechanobiological cues (mechanical properties match with mechanobiological signaling), adding biochemical cues, i.e., biomolecules, and being permissive to cells so that they can locally migrate in and remodel their surroundings. For example, for cells to maintain their health and viability during the bioprinting process, the ink material (s) should be cytocompatible and protect cells. Shear stress, pressure and temperature changes, UV light, and long process duration without replenishment of nutrients can damage the viability of cells [52].

Designing biomimetic bioink, i.e., cell-laden biomaterial, is still a challenge because many material properties that are required for processability and shape fidelity can conflict with those required for cell survival and directed growth. Self-healing dynamic materials have been developed to overcome those problems [52]. The bioink properties should mimic those of native ECM. Fig. 2 shows the evolution of bioinks from traditional statically crosslinked hydrogels to dynamic bioinks toward mimicking the native ECM. In static bioink (Fig. 2 (a)), cells cannot behave like in a native ECM, whereas in degradable network (Fig. 2 (b)), they can already rearrange more naturally and move around, although the environment change is irreversible [52,53]. There would be a need for dynamic hydrogel (Fig. 2 (c)), able to deliver bioactive molecules over time but also respond to cellular behavior. Further, dynamic hydrogels (Fig. 2 (d)) could mimic the native ECM by allowing a dynamic responsive environment for cells to reside in, but also contain biomechanical and biochemical cues [52].

2.2.1. Dynamic microenvironment

Stem cells reside *in vivo* in special microenvironments, also called the stem cell niche, which has both biochemical and biophysical factors directing resident stem cell fate, and which is both complex and dynamic [54]. The niche consists of ECM molecules, soluble proteins (e.g., cytokines, growth factors), and supporting cells [55]. Stem cell behavior is modulated by the microstructure, mechanical properties and biochemical composition of the ECM, depending on the stem cell type and desired phenotype. The behavior of stem cells is also affected by the cell–cell interactions within the niche. Stem cell fate can be controlled either by maintaining stem cell phenotype (stemness) or by differentiating stem cell into desired mature cell types [54]. Stem cells also influence the niche either by exerting mechanical forces through their cytoskeletal components or by secreting bioactive molecules [55]. Thus, there is a dynamic interaction between niche components and stem cells.

Native tissues are viscoelastic and have time-dependent mechanical properties [56,54]. The mechanical properties of ECM can alter cells' ability to generate tension by modulating cell spreading, nuclear shape, and intercellular signaling pathways [54]. To mimic these properties, hydrogels have been designed with tunable viscoelasticity [57,58]. Different cell types require different kinds of microenvironments for proper growth, differentiation, elongation, and migration. For example, neuroblasts are prone to neural differentiation in hydrogels with lower stiffness (0.1–1 kPa), whereas on stiffer hydrogels (7–10 kPa), they are prone to glial differentiation [59–62]. Thus, the modulation of 3D-stiffness of the construct would be desired, although the mesh size and swelling properties can change too [54].

Since ECM stiffness has been found to play an important role in the directional differentiation of stem cells, it should be taken into account when designing self-healing hydrogels [18]. The challenge is to create a suitable environment with mechanical and biological cues promoting mechanotransduction (i.e., the cell's capacity to transduce intercellular molecular interaction into forces influencing the properties and architecture of the microenvironment, or external forces into biological signals to induce selected cellular functions [55]) and mechanosensing (i.e., the cells' capacity to sense mechanical forces and physical cues from the surrounding environment [55]) signals for the guidance of stem cell activity and fate [18,54]. Studies with dynamic networks have also shown that the materials' time-dependent response, i.e., modulation of the materials' biochemical, physicochemical, and mechano-structural (e.g., elasticity, topography) properties over time, is important because that has an effect on cellular function and fate [52,63,64]. Because we know that *in vivo* cellular microenvironments are not static (their physicochemical properties gradually change), *in vitro* platforms capable of recapitulating dynamic *in vivo* signaling would advance TE [63].

From a biological point of view, the advantage of using self-healing shear-thinning hydrogels as bioinks is due to their ability to adapt to the needs of the cells growing inside them, i.e., to respond to cell forces so that the bonds can break and reform, and the network can rearrange, but at the same time, bulk biophysical properties remain constant [15]. Thus, the cells can spread more within the dynamic network compared to the static counterpart [10,65]. As the cells spread, bonds are broken, but on the other hand, more are formed. In this way, the growth conditions remain more stable than in traditional hydrogels [15]. Traditional hydrogels having static networks and low mechanical strength, can be prone to breakage and lose their properties, as well as lack the needed dynamics for matrix remodeling and cell expansion [18,66,53]. As self-healing hydrogels can autonomically and intrinsically heal their damages and restore the original properties and shape due to their

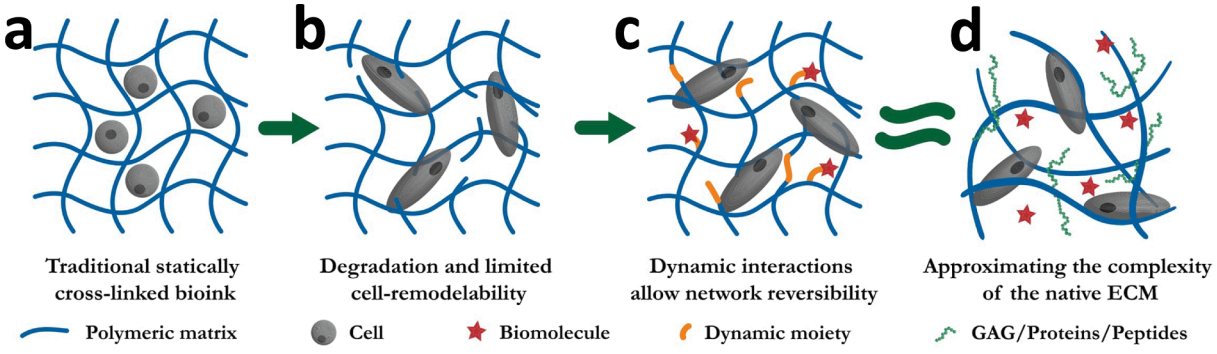

Fig. 2. Bioink evolution towards mimicking the native ECM: (a) statically crosslinked bioink, (b) degradable network, (c) dynamic hydrogel with bioactive molecules, and (d) dynamic network mimicking the complexity of the native ECM. Reprinted with permission from Morgan et al. (2020) [52] Copyright ©2020 Wiley. Online Library.

dynamic reversible bonding, they can also protect encapsulated cells by dissipating compressive and shear forces if used for injection/extrusion [18,53,67].

Self-healing hydrogels can also be flexible and permeable, which can enhance nutrient exchange and increase cell viability [18,66]. Also, due to their physical and chemical dynamism, the growth, fate, and behavior of cells can be controlled [18,53]. Permanently crosslinked hydrogel structure may be an inadequate niche for stemness maintenance, whereas advances in self-healing hydrogels together with stem cell niche design principles can be used to prompt the wanted stem cell phenotype for specific application [18]. Thus, while traditional static hydrogels can only minimally regulate and guide cellular behavior or cell fate within the microenvironment, self-healing hydrogels play a greater role in that [18].

Ink formulation should be biocompatible, cytocompatible, and have high cell viability [3]. Regulation or guiding of cell behavior and fate is usually done by designing the surface/interface of materials or functionalization with bioactive molecules (e.g., proteins and polysaccharides naturally present in ECM, or peptides), which can, however, change the shear-thinning behavior and mechanical properties of the bioink. Therefore, those should be optimized before printing [2,50,53,18]. More recently, dynamic physical cues have found to affect in cell spreading, expansion, migration and differentiation, as well as stemness maintenance and regulation of cell secrotome [53].

2.2.2. Stress relaxation

Stress relaxation is also an important mechanical property to be considered. Native ECM is not only dynamic and remodellable but has stress relaxation property. Static traditional hydrogels have finite stress relation and cannot be remodeled if not degradable. Dynamic hydrogels with self-healing, shear-thinning, and fast stress relaxation properties, on the other hand, can provide the needed dynamic physical cues (dynamic elastic modulus) for cells [53]. For example, ionic and covalent hydrogels have stress relaxation property. In ionic gels, stress relaxes mainly through breaking/reforming of the ionic crosslinks, and the time scale of relaxation does not depend on the sample size, while in covalent hydrogels, stress relaxes mainly through the migration of water, and as the sample size increases, the relaxation slows down. [68] Compared with covalent hydrogels, the stress relaxation is faster and modulation is easier with ionic gels [69]. Also, for example, in the case of dynamic hydrazone crosslinked hydrogels, it has been shown that the stress relaxation rates are faster when using aliphatic aldehydes compared to aromatic aldehydes [65].

By using dynamic bonding with tunable stress relaxation in hydrogels, like in the study by Lou et al. [70], a more biomimicking environment in terms of mechanical and structural cues can be achieved. They, for example, showed that faster relaxation in their hydrogels promoted cell spreading, fiber remodeling, and focal adhesion formation. [70] Dynamic hydrogel's stress relaxation contributes to biophysical signals to integrin, thus guiding cell spreading and expansion, whereas a static mechanical environment inhibits them and focal adhesion formation [53,70]. Faster stress relaxation of hydrogels has also been related to chondrogenesis differentiation, i.e., stress relaxation altered chondrocyte phenotype matrix deposition, as it modulates cell volume expansion [71].

Material cues, such as stress relaxation, stiffness, or degradability, can regulate stem cell function [72]. Pathways that are activated by these cues are, for example, Rho/ROCK (Rho protein/Rho-associated kinase) that is needed for YAP (yes-associated protein) and TAZ (WW domain-containing transcription regulator) transcription factor activity [53,72]. When cells are cultured in stress-relaxed dynamic hydrogels, YAP/TAZ is activated and they present cell volume expansion and spread [53,73]. As an example, Fig. 3 (a) shows the stress relaxation behavior of elastic, irreversible covalent bonding hydrogels, stress-relaxing reversible bonding hydrogels, and native collagen. It also illustrates the difference between static and remodelable dynamic stress-relaxed environments (Fig. 3 (b)). In Fig. 3 (c), the inhibition or activation of YAP/TAZ in both environments is shown. It also shows the rate of stress relaxation on the maturation of FA and F-actin remodeling.

2.2.3. Yield stress

When combined with shear-thinning behavior and fast recovery,

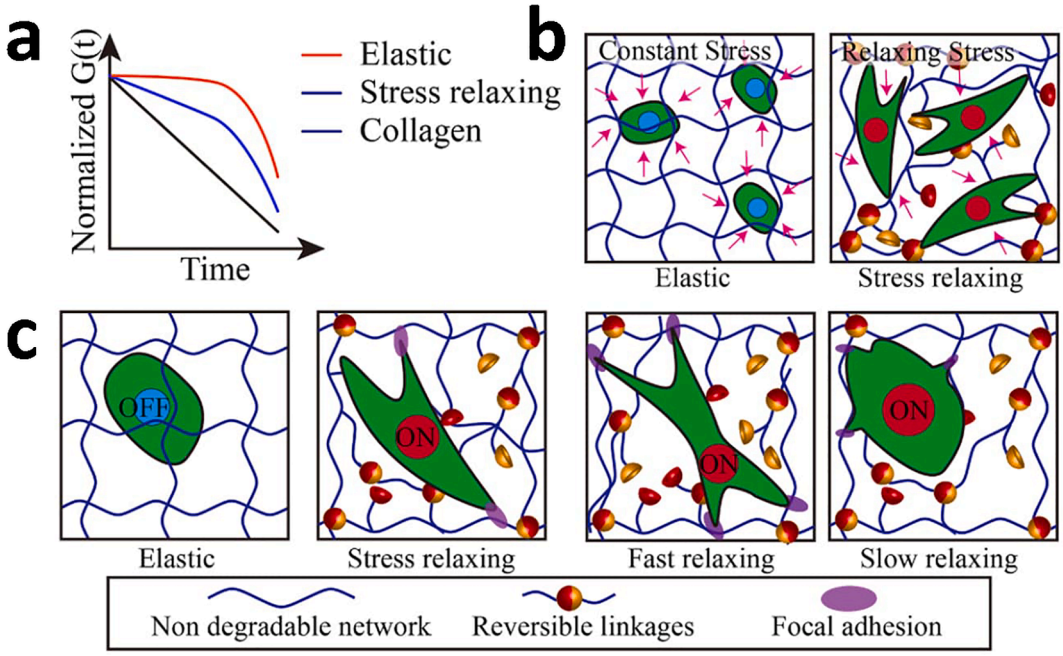

Fig. 3. (a) Stress relaxation of elastic hydrogel (irreversible bonds), stress-relaxing hydrogel (reversible bonds), and native ECM collagen. (b) Elastic hydrogel with static mechanical environment and fixed architecture, and stress-relaxing hydrogel with dynamic mechanical environment and remodelable architecture. (c) Inhibition (OFF) and activation (ON) of YAP/TAZ in elastic and stress-relaxing hydrogels, respectively, and the effect of stress relaxation rate on maturation of FA and F-actin remodeling. Reprinted with permission from Tong et al. (2021) [53] Copyright ©2021 Elsevier.

bioinks featuring yield stress inherently resist deformation, ensuring the preservation of the printed structure, which is a pivotal benefit for 3D-bioprinting [42]. For example, there is a study [74] highlighting the benefits of bioinks with yield stress in maintaining shape fidelity and preventing cell sedimentation. They also emphasized the superiority of yield stress over high viscosity, as it prevents deformation rather than merely delaying it. While yield stress is advantageous, achieving high print fidelity also relies on the complementary interplay of shear-thinning performance and suitable recovery time. [74] Another study [75] further emphasized these three parameters, particularly in chondroitin sulfate-based hydrogel printing, stating that their presence still allowed tailoring of characteristics like porosity for cell encapsulation. Generally, a yield stress above 100 Pa is recommended for optimal print fidelity, although bioinks below this threshold may still be printable [42]. However, too high yield stress could necessitate very large pressures (not achievable using current extruders) and potentially lead to significant cell death, highlighting the importance of balancing these factors [76]. Thus, the hydrogel's rheological properties, including yield stress, directly impact the viability of loaded cells during the bioprinting process: high yield stress may subject cells to shear forces and mechanical stress during extrusion, whereas optimal yield stress allows for gentle extrusion of the bioink, minimizing shear stress on the cells and preserving their viability.

2.2.4. Shear-thinning property

In the case of EBB, shear-thinning property plays an important role since the viscosity is reduced under applied shear and can prevent cell sedimentation [18,38,77]. Shear-thinning hydrogels can also protect cells from the stress caused by the extrusion/injection because of the shear banding and plug-flow velocity profiles that limit cellular membrane disruption during shear flow [5,37]. In addition to the shear-thinning property of bioink, the shear stress experienced by the cells in EBB can be altered by nozzle modality and diameter, printing temperature, extrusion pressure, and polymer concentration [45]. Shear-thinning hydrogels with controlled *in situ* stiffening ("shear-thinning hydrogels for injectable encapsulation and long-term delivery aka SHIELD") can also regulate stem cell secrotome, which in turn has an important role in cell behavior and fate [53,78].

2.2.5. Recovery time

Recovery time dictates how easily the cells can be incorporated. For example, too quickly recovered materials would result in heterogeneous cell distribution since mixing in cells is difficult. Also, too slow recovery time would result in heterogeneous cell distribution, cell sedimentation, and poor shape retention. [42,79]

2.2.6. Vascularization and innervation

Vascularization is important for bioprinted constructs since constructs with over 200 μm thickness need vascularization to transport nutrients, oxygen and waste [48,13]. Dynamic hydrogels are good candidates in terms of vascularization. For example, Hsieh et al. [80] were able to form capillary-like structures using vascular endothelial cells-seeded chitosan-fibrin-based self-healing hydrogels. Hydrogel alone was also shown to promote angiogenesis and rescue blood circulation when injected in zebrafish or mice, respectively. [80] Vasculatures can also be bioprinted either by using direct or indirect bioprinting, i.e., printing channels using sacrificial bioprinting and endothelialization [13]. For example, Wang et al. [81], inspired for example by the gel-in-gel bioprinting study by Highley et al. [47], fabricated microvascular construct by directly printing alginate into agarose, gelatin, or gelatin methacrylate (GelMA) pre-polymers of hydrogel (support bath) that also contained calcium (Ca^{2+})-crosslinker. After printing, pre-polymers could be returned to a steady state by adding stimulus (temperature, enzyme, or UV-light), whereas printed alginate can be liquified and removed. Additional endothelialization was also used. [81] Section 3.2 also presents a previous study by Fang et al. [82] in which a new bioprinting strategy called sequential printing in a reversible ink template (SPIRIT), together with shear-thinning self-healing microgel-based biphasic bioink, can be used to bioprint a ventricle model with a perfusable freeform vascular network [82].

Innervation, on the other hand, is needed for the proper function and integration of implanted constructs with the host tissue. Vascularization and innervation are actually considered functionally coupled, as many times blood vessels and nerves follow the same paths. [83,84,3] For example, Tseng et al. [59] used glucose-sensitive self-healing hydrogels as sacrificial materials to form branched tubular channels within the construct (non-glucose-sensitive hydrogel with neural stem cells), and seeded endothelial cells in the channels. Vascularized neural tissues were formed, i.e., endothelial cells formed a vascular network, while neural stem cells formed a neurosphere-like structure in the construct. [59] The limiting factor in combining vascularization and innervation has been the problem of how to supply a universal medium to both neurons and vascular cells that could sustain both phenotype maturation and development [85,3]. Overall, the combination of vascularization and innervation should be studied more in 3D-bioprinting applications in order to achieve better functioning and biomimicking constructs.

2.2.7. Effect of cells on the bioink properties

Not only does the bioprinting process affect cells, as already mentioned, but also the cells affect the properties of bioink. For example, cell density influences the behavior of ECM production and cells, and therefore also the structure and function of the bioprinted construct. In general, faster formation of tissue and better cell–cell interactions can be achieved using higher cell content, although the viscosity and printability of the bioink may be affected [13,28]. For example, there are studies showing that the viscosity of the bioink increases as the cell density increases, but also some opposite results where viscosity, yield stress, G', and gelation kinetics decrease when cell density increases [86–91]. Anyway, more studies with different crosslinking chemistries and cell densities, as well as cells with different metabolic activity, are needed to understand why the properties of the bioink change. Also, how to find a balance between resulting viscosity, cell density, and cell–cell- and cell-material interactions remains a challenge in the field. [45]

3. Self-healing hydrogels in 3D-bioprinting applications

The most common printing method for self-healing and shear-thinning hydrogels is EBB. Both covalent and physical crosslinking methods have been used for EBB. However, despite the number of self-healing crosslinking methods, only few of them have been used for 3D-bioprinting suitable for biomedical applications. In case of self-healing covalently crosslinked hydrogels, imine and hydrazone crosslinking are mainly used. In case of extrudable supramolecular hydrogels, crosslinking methods like guest–host interactions, coordination bonding, peptide-peptide interactions and hydrophobic interactions have been used. In order to get more mechanical stability for the printed structure, many times also a secondary post-crosslinking has been used. Other less used 3D-(bio) printing methods for self-healing hydrogels are inkjet printing and stereolithography. The next sections present some of the most relevant studies from recent years related to covalently crosslinked and supramolecular self-healing hydrogels for EBB, as well as for inkjet- and stereolithography-based bioprinting.

3.1. Covalently crosslinked self-healing hydrogels for extrusion-based bioprinting

This section presents some of the most relevant studies of recent years related to covalently crosslinked self-healing hydrogels for EBB. All the presented hydrogels are also collected in Table 1.

Wang et. al. [92] studied self-healing and shear-thinning hyaluronan (HA)-based hydrogels crosslinked through hydrazone chemistry suitable

Table 1
Covalently crosslinked self-healing hydrogels for extrusion-based bioprinting.

Crosslinking type	Hydrogel components	Printer	Printing specifications	Printing results	Cell viability %	Ref.
Hydrazone (+UV-photocrosslinking after printing)	Hydrazide-modified HA (HA-HYD) + Aldehyde-modified HA (HA-ALD)	A commercial 3D Fused Deposition Modeling printer (Revolution XL, Quintessential Universal Building Device)	Needle gauge: 18, 23, 25 G, Extrusion force: 1 to 18 N	Force increased with increasing needle gauge or material concentration, filament diameter (around 1300 to 500 μm) decreased with increasing needle gauge, 4 layer lattice stable after printing	Mouse embryonic NIH 3T3 fibroblasts: after printing ≈85%, before printing ≈95%, viability affected by the printing parameters	[92]
Hydrazone	Oxidized alginate (ox-alg) + adipic acid dihydrazide (hydrazone)	A BioScaffolder (GeSiM-Gesellschaft *für* Silizium-Mikrosysteme mbH, Radeberg, Germany)	Needle gauge: 25 G, Printing pressures: 115,120 and 140 kPa, Speed: 5, 6 and 7 mm/min	1, 2 and 4 layered grid structures, name "MERLN" and a vascular tree model, 5 mm/min and lower pressures were most optimal	Mouse teratocarcinoma ATDC5 cells: slightly decreased viability after 24 h of bioprinting	[15]
Schiff-base (+UV-photocrosslinking after printing)	Chitosan-starch + dialdehyde debranched starch (DADBS)	A robotic deposition device (Foodbot-E1, China)	Speed: 30 mm/s	Different shapes (mice, starfish, octopus, and letters)	No cell tests were conducted	[93]
Schiff-base (+blue light-photocrosslinking after printing)	Phenol-functionalized chitosan (Chi-Ph) + dibenzaldehyde-terminated telechelic poly(ethylene glycol) (DF-PEG)	A syringe + needle	Needle gauge: 23 G	Tube-like block, and Y-like constructs	hMSCs: A homogeneous distribution of hMSCs in the printed filaments of a lattice structure, hardly any dead cells inside of them, but several dead cells on the filaments' edges	[44]
Schiff-base (+stable amide bond)	Aldehyde hyaluronic acid (AHA)/N-carboxymethyl chitosan (CMC) + gelatin (GEL)/4-arm poly(ethylene glycol) succinimidyl glutarate (PEG-SG)	A bioprinter (Livprint Norm, Medprin, China)	Needle gauge: 25 G, Interlayer offset: 90°, Infill rate: 30%, Linear peed: 6 mm/s, Extrusion speed: 0.07 mL/min, Temperature control off	Grid structures with continuous filaments of about 0.46 mm diameter, multiple-sample and larger sample printing also possible,	NIH/3T3 cells: around 90 % (day 21) + *in vitro* nerve-like (NE-4C), muscle-like (C2C12), and cartilage-like (chondrocyte) constructs: homogeneous cell growth	[94]
Schiff base	Glycol chitosan (GC) + oxidized HA-adipic acid dihydrazide (OHA) + superparamagnetic iron oxide nanoparticles (SPIONs)	A 3D bioprinter (Invivo, Rokit, Korea) equipped with a pressure-controlled cartridge	Needle gauge: 25 G, Moving speed (nozzle): 3 mm/s to 7 mm/s	Filaments (diameter decreased (around 1 to 0.6 mm) with increasing printing speed (5 mm/min was optimal)), model objects with various shapes (constructs could transform their shape under magnetic field)	ATDC5 cells: around 90 to 100 % (48 h)	[95]
Schiff base + acylhydrazone	Oxidized hyaluronate (OHA) + glycol chitosan (GC) + adipic acid dihydrazide (ADH) + superparamagnetic iron oxide nanoparticles (SPIONs)	A 3D printer (Invivo, Rokit; Korea) equipped with a pressure- controlled cartridge	Needle gauge: 25 G, Printing speed: 60 to 420 mm/min	Filaments: increasing speed results in a thinner filament diameter (around 0.7 to 0.4 mm, 180 mm/min was optimal printing speed), Construct: a dynamic scaffold system of ferrogel gel + non-ferrogel	ATDC5 cells: around 75 to 80 % (day 7)	[96]
Schiff base + acylhydrazone	Oxidized hyaluronate (OHA) + glycol chitosan (GC) + adipic acid dihydrazide (ADH)			Different shapes (i.e. donut, disc, meniscus shapes) with various volumes and heights, and unitary objects with fused filamentous layers	ATDC5 cells: more than 80% (one week), cells did not affect to self-healing properties	[97]
Schiff base + acylhydrazone + ionic	Oxidized hyaluronate (OHA) + glycol chitosan (GC) + adipic acid dihydrazide (ADH) + alginate (ALG) + $CaCl_2$	A 3D printer (Invivo, Rokit; Seoul, Korea)	Motor pressure: 300 N, Needle gauge: 25 G, Printing speed: 8 mm/min, Temperature: 25°C	Filaments: stacking of fibers layer-by-layer lead to laminated structure without any collapse and further self-healing resulted a single structure, Construct (including cells): different shapes, $CaCl_2$ addition enhanced the mechanical stiffness and stability	ATDC5 cells: over 95 % in hydrogel components and in hydrogel after printing with or without calcium	[98]
Boronate ester bond + ionic	Phenylboronic acid modified alginate (Alg-PBA) + poly (vinyl alcohol) (PVA) + $CaCl_2$	A Bioplotter 3D (EnvisionTEC, Dearborn, MI, USA)	Needle gauge: 22 G and 25 G, Printing pressure: 2.00 ± 0.3 bar, Printing speed: 8 mm/min	Filaments: the thickness was 700 μm on average (22 G nozzle) and 300 μm on average (25G nozzle), Grid and cylindrical structures with good structural fidelity (22G nozzle)	Mouse chondrocytes: over 85% (7 days) & scaffolds reduced oxidative stress for embedded cells under hydrogen peroxide exposure	[99]

for extrusion-based 3D-printing with high shape fidelity and stability for relaxation. These type of hydrogels have previously been shown to be suitable for injectable applications, i.e., being cell protective when extruded through a needle [67]. Also, in this case, injectability through a syringe and a needle was proved. Material concentration (1.5, 3, 5 wt.%) and needle gauge (18, 23, 25 G) determined the filament sizes and forces for extrusion, i.e., the force increased (around 1 to 18 N) with increasing needle gauge (fixed concentration), whereas the force increased with increased concentration (fixed needle gauge). A stable force profile was achieved with the largest needle and lowest concentration. Filament diameter decreased (around 1300 to 500 μm) with increasing needle gauge. However, highest concentration lead to fractured filaments with inconsistent size. Also, multilayered structures, i.e., 4-layer lattice, were printed and shown to be stable after printing in air and in phosphate buffered saline (PBS) (some swelling and increased filament diameter over time). Printing parameters affected the cell (mouse embryonic NIH 3T3 fibroblasts) viability, i.e., the lowest concentration and needle gauge (i.e., lowest force) lead to best viability, further indicating that force has a direct impact on cell viability during printing. Higher resolution could be achieved using smaller needles, which, however, decreased cell viability. The cell viability after printing was high (≈85%), close to that before printing (≈95%). A photostiffening (double-networks of HA-based hydrogels with photocrosslinkable norbornene-modified HA and crosslinker) and photopatterning (rhodamine-dextran encapsulated) were used to increase the functionality of the scaffold, i.e., decreased filament erosion and increased modulus of the scaffold were achieved with photostiffening, and spatial modification of scaffolds with dyes was shown possible (photopatterning). [92]

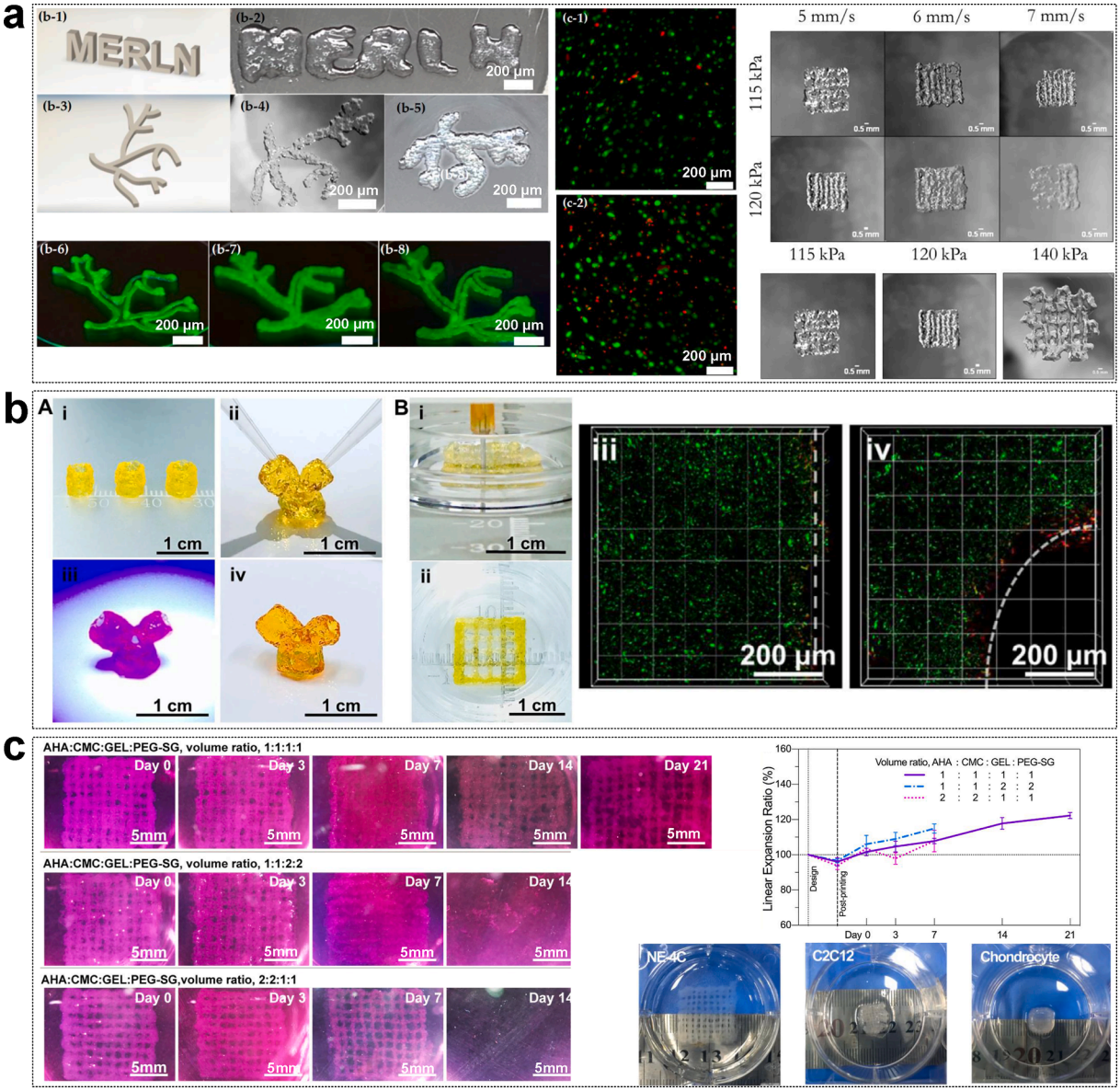

Fig. 4. Extrusion-based bioprinting of covalently crosslinked hydrogels. (a) Letters "MERLN" and vascular tree structure (b1-8) printed using hydrazone-based alginate hydrogel inks, live/dead staining of ATDC5 cells after 24 h without printing (c-1) or after bioprinting (c-2), and printability studies using different speeds and pressures (2-layered structures, 25 G needle, 5 mm/min) [15]. (b) 3D-printed tube-like components (Ai) assembled as Y-like constructs (Aii-iv) using imine-based CPDP hydrogel inks, further irradiated with blue light (60 s) (Aiii), bioprinting of hMSC-laden photocrosslinkable hydrogel inks (Bi-ii), and live/dead-staining of hMSCs in the filament (Biii) and intersecting filaments (Biv) after 4 h (filament border = white dashed lines) [44]. (c) Integrity studies of printed cell-free imine-based AHA/CMC/GEL/PEG-SG hydrogel constructs (subaqueous images during incubation), print fidelity and dimensional change profiles of the cell-free constructs, and *in vitro* tissue-like (NE-4C, C2G12 and Chondrocyte) constructs after 21 days of culture [94]. Reprinted with permission from Hafeez et al. (2018) [15] Copyright ©2018 MDPI, Liu et al. (2021) [44]Copyright ©2021 Elsevier, and Chen et al. (2021) [94] Copyright ©2021 Elsevier.

Hafeez et al. [15] (Fig. 4 (a)) developed a small library of self-healing bioprintable hydrogels from oxidized alginate (ox-alg) with different crosslinkers (adipic acid dihydrazide for hydrazone and hexamethylene disemicarbazide for semicarbazone) to be used as dynamic 3D-cell culture systems, for therapeutics and cell delivery, and as smart bioinks for soft TE. No additional crosslinking was needed. The self-healing of hydrazone was about 30 min while with semicarbazone it was about 10 min. Also, a two-phase healing recovery was seen. Based on initial injectability test, semicarbazone needed a larger needle diameter and higher pressure, so hydrazone was considered more suitable for cells and bioprinting. Different deposition speeds and extrusion pressures on printability were tested. 2-layered grid structures using a 25 G needle were printed (using 115 and 120 kPa pressures) resulting in more homogeneous structures with 5 mm/min speed compared to 6 and 7 mm/min. The highest pressure was optimal for fiber extrusion with 5 mm/min when different pressures (115, 120 and 140 kPa) were tested. With optimized parameters, 1, 2 and 4-layered grid structures could be created, although with no high fidelity. Also, more complex structures, with 6 mm thicknesss, i.e., letters "MERLN" and a vascular tree model were printed, although with the name, the sharp angles and parallel or closely spaced lines resulted in merging and occlusion. By using manual disruption of the gel network before printing lead to more uniform material deposition and better resolution vascular structure. After 24 h of bioprinting, the viability of mouse teratocarcinoma ATDC5 cells decreased a little (compared to the control without printing), perhaps due to the shear stress during printing. [15]

Liu et al. [93] introduced a new type of crosslinker, dialdehyde debranched starch (DADBS), to prepare rapidly gelated (< 30 s) dynamic Schiff-based chitosan-starch hydrogels having adjustable mechanical properties and elasticity. DADBS is biodegradable and safe compared with conventional crosslinkers like glutaraldehyde. These hydrogels had rapid self-healing ability (< 30 min), and great fluorescence properties. Their good 3D-printability using extrusion-based 3D-printing enabled the printing of different shapes (mice, starfish, octopus, and letters). Despite no cell tests were conducted, these hydrogels can hold great potential, for example, in medical applications. [93]

Liu et al. [44] (Fig. 4 (b) Ai-iv and Bi-iv) studied chitosan-based self-healing hydrogels to be used as bioink, particularly for modular 3D-bioprinting. The hydrogel (CPDP) was formed from phenol-functionalized chitosan (Chi-Ph) and dibenzaldehyde-terminated telechelic poly (ethylene glycol) (DF-PEG) and was based on imine-crosslinking (reversible bonds) and secondary visible light-crosslinking (irreversible phenol-phenol-bonds). Suitability for modular 3D-printing was preliminary proven by showing instantaneous adhesion as well as interface healing between printed CPDP constructs. Actual modular printing was proven by printing CPDP hydrogels through a 23 G needle to be used as individual building blocks (tube-like, Ai) that could be assembled into more specific Y-like constructs (Aii). The contacting interfaces healed in a few seconds, and secondary photocrosslinking (Aiii) was used for further reinforcement. Additionally, human mesenchymal stem cells (hMSCs)-laden CPDP hydrogel was bioprinted through a 23 G needle and further photocrosslinked (Bi-ii). A homogeneous distribution of hMSCs in the printed filaments of a lattice structure was shown, as well as hardly any dead cells inside them (Biii). However, there were several dead cells on the filament edges (Biv). Liu et al. suggest, however, that the cells could be secured better during the printing process by decreasing the materials' yield stress and adjusting the printing parameters, like needle size, printing speed, or extrusion rate. Thus, this modular 3D-bioprinting using CPDP hydrogels could be suitable for building large-sized constructs with a heterogeneous structure and a specific shape as well as multiple cell types to mimic soft tissues. [44]

Chen et al. [94] (Fig. 4 (c)) introduced a time-sharing structure-supporting hydrogel composed of fast crosslinking aldehyde hyaluronic acid (AHA)/N-carboxymethyl chitosan (CMC) and slow stable crosslinking gelatin (GEL)/4-arm poly(ethylene glycol) succinimidyl glutarate (PEG-SG) to be used as bioink for EBB for TE and targeted cell therapy. These hydrogels self-healed in 10 min at room temperature. Grid structures with continuous filaments of about 0.46 mm diameter were able to print. Also multiple-sample and larger sample printing was possible. Fast crosslinking enables immediate printing after the preparation of formulation due to its self-healing ability and slow crosslinking gives structural stability during printing. Chen et al. also showed the structural durability and stability of the printed constructs by transferring them in Dulbecco's Modified Eagle Medium (DMEM) cell culture medium for 21 days. 6 layered grid structures with NIH/3T3 cells were also printed. The viability on day 21 was around 90 %. Additionally, *in vitro* nerve-like (NE-4C), muscle-like (C2C12), and cartilage-like (chondrocyte) constructs were printed that showed homogeneous cell growth. [94]

Ko et al. [95] studied magnetically responsive self-healing glycol chitosan (GC)-oxidized HA-adipic acid dihydrazide (OHA) hydrogels that contained superparamagnetic iron oxide nanoparticles (SPIONs). The printability of these ferrogels via an extrusion-based printing method was studied by changing the moving speeds of the nozzle (3 mm/s to 7 mm/s) and the platform and the input flow through a fixed nozzle. With a 25 G needle (nozzle), filament diameter decreased (around 1 to 0.6 mm) with increasing printing speed resulting in breaking of the filament at speed higher than 6 mm/min in the end, so 5 mm/min was considered optimal. Further, 3D-printed constructs showed an ability to transform their shape under magnetic field. The original shape could be restored upon removal of the magnetic field and repeated this several times. This could indicate their potential use in 4D-printing. No cytotoxicity of the hydrogel components or either hydrogels of the system (viability around 90 to 100 % on 48 h) was observed when tested with ATDC5 cells. Thus, these hydrogels hold great potential for TE, but also for drug delivery systems. [95] Choi et al. [96] (Fig. 5 (a)) also studied the same systems combining self-healing hydrogels and self-healing ferrogel without the need of post-crosslinking. The printability of these ferrogels via an extrusion-based method were tested by varying the printing speed (60 to 420 mm/min). As the printing speed increased, the filament diameter was shown to become thinner (around 0.7 to 0.4 mm). However, at a printing speed higher than 300 mm/min, the filament was disconnected, so 180 mm/min was selected as the optimal speed. A dynamic scaffold system of ferrogel gel and non-ferrogel was printed to show its suitability for TE under repeated magnetic stimulation. Also, the viability of ATDC5 cells (around 75 to 80 % on day 7) in both hydrogels of the system were shown to support this. [96]

Kim et al. [97] combined two dynamic bonds, namely acylhydrazone and imine crosslinking, to fabricate oxidized hyaluronate (OHA)/glycol chitosan (GC)/adipic acid dihydrazide (ADH) hydrogels for use as bioink in EBB for TE applications, including cartilage regeneration. The hydrogel's self-healing ability and mechanical properties enabled the stacking of the gel as a bioink, allowing for the fabrication of different shapes (e.g., donut, disc, meniscus shapes) with various volumes and heights. There was no need for additional crosslinking. Additionally, unitary objects with fused filamentous layers were able to fabricate due to self-healing ability. Encapsulated ATDC5 cells did not affect the self-healing properties of the hydrogel, and their viability was maintained after printing with more than 80% viability after incubating for one week. [97] Roh et al. [98] (Fig. 5 (b)) used the same OHA/GC/ADH hydrogels with additional alginate and calcium ions, resulting in a dual crosslinking system to be used as bioink for EBB for similar applications. The printability was tested by applying strong shear force during printing, which resulted in breaking of the gel structure, although the gel self-healed immediately and kept the fiber form. The stacking of fibers layer-by-layer lead to a laminated structure without any collapse, and further self-healing resulted in a single structure. The addition of calcium chloride enhanced the mechanical stiffness and stability. 3D-constructs with ATDC5 cells were also printed in different shapes. The viability of cells was over 95 % in hydrogel components and in hydrogel after printing with or without calcium, which indicates that the printing

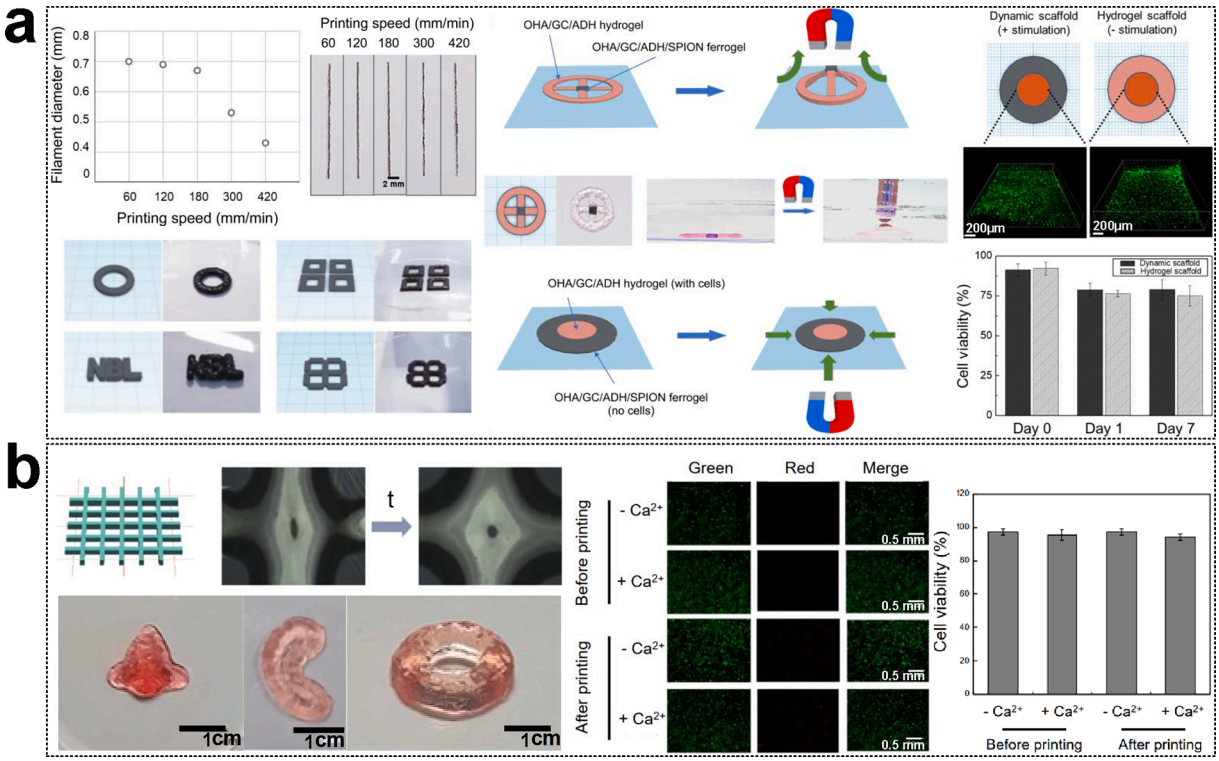

Fig. 5. Extrusion-based bioprinting of covalently crosslinked OHA/GC/ADH/ALG-based hydrogels. (a) Filament diameter based on the printing speed and different 3D-structures printed with imine-based OHA/GC/ADH/SPIONs-ferrogels, response of OHA/GC/ADH-OHA/GC/ADH/SPION ferrogel under magnetic field, 3D-printed OHA/GC/ADH (cells)-OHA/GC/ADH/SPION ferrogel (no cells, dynamic scaffold)-based construct, and live/dead staining of ATDC5 cells cultured in dynamic or hydrogel scaffolds 7 days post-culture and cell viability (%) over time under magnetic stimulation [96]. (b) 3D-printed filaments and 3D-printed constructs of different shapes using acylhydrazone-, imine & ionically-crosslinked OHA/GC/ADH/ALG hydrogel inks, and live/dead staining of ATDC5 cells and cell viability (%) before and after printing (with or without calcium ions) [98]. Reprinted with permission from Choi et al. (2021) [96] Copyright ©2021 Elsevier, and Roh et al. (2021) [98] Copyright ©2021 MDPI.

process or the secondary crosslinking do not affect cell viability. These hydrogels also provided a microenvironment suitable for chondrogenic differentiation of ATDC5 cells *in vitro*. [98]

Zhang et al. [99] fabricated self-healing, shear-thinning alginate-based hydrogels using dynamic covalent bonding between the phenylboronic acid modified alginate (Alg-PBA) and poly (vinyl alcohol) (PVA) to be used as bioink for EBB for cartilage TE. Since there is a lack of multifunctional bioinks that can not only support the differentiation and growth of cells but also protect cells against injuries caused by elevated oxidative stress, these bioinks were designed to also have anti-oxidative properties. Grid and cylindrical structures with good structural fidelity were achieved. After stabilizing the gel with additional ionic crosslinking, the long-term growth of mouse fibroblasts was shown. Also, the viability of mouse chondrocytes remained high for 7 days, but more importantly, these scaffolds were shown to reduce oxidative stress for embedded chondrocytes under hydrogen peroxide (H_2O_2) exposure. [99]

3.2. *Supramolecular self-healing hydrogels for extrusion-based bioprinting*

This section presents some of the most relevant studies in recent years related to supramolecular self-healing hydrogels for EBB. All the presented hydrogels are also compiled in Tables 2 and 3.

Hydrogels formed using guest–host crosslinking can be used in injectable applications or as bioink in 3D-printing applications due to their shear-thinning ability when injected through a syringe and self-healing ability (within seconds) when shear forces are removed [100]. The limitation of conventional EBB is that the deposition of discrete layers is difficult since they are not mechanically supported by the layers underneath [112]. Highley et al. [47] (Fig. 6 (a)) proposed a new approach to overcome this by using gel-in-gel bioprinting, i.e., direct printing of shear-thinning hydrogels into self-healing support hydrogel. More specifically, they used guest–host crosslinked HA-based hydrogels (adamantine-modified HA (Ad-HA) and β-cyclodextrin-modified HA (CD-HA)) as printable and support materials because the bonds can be disrupted by applying a physical stimulus like shear stress and reformed after removing the stimulus. In case of the support hydrogel, its self-healing ability makes it possible to heal around the printed ink after injecting the other gel with the syringe needle, and likewise, the printed ink retains its structure in the support. The printed ink could be extruded through a variety of needle diameters and maintain printing fidelity after printing in support. The support hydrogel was shown to be shear-yielding and self-healing, but most importantly, resistant to deformation from needle motion. This kind of bath system makes continuous printing possible in any direction in 3D-space, for example, printing spiral structures, as well as multiple inks and structures (spirals and filaments) in the same support. MSCs and 3T3 fibroblasts were also printed in printed gel, support, or both to form patterned multicellular structures. The printing process was not affected by the inclusion of cells and was found to be nontoxic to cells (viability >90%). Secondary stabilization of support or ink using photocrosslinking (methacrylates introduced into HA) was also tested since they may lack long-term stability or perfusion. In this case, freestanding pyramidal 3D-structures (ink stabilized) or channels (support gel stabilized) were able to be formed using this method which is based on the removal of the unstabilized gels. [47]

Loebel et al. [100] investigated similar hydrogels using the same gel-in-gel printing method. For example, a continuous spiral around another one was printed in a support bath. Encapsulated cells (MSCs and 3T3 fibroblasts) were shown to have high viability in the extruded material

Table 2
Supramolecular self-healing hydrogels for extrusion-based bioprinting. (1/2)

Crosslinking type	Hydrogel components	Printer	Printing specifications	Printing results	Cell viability %	Ref.
Guest–host(+UV-photocrosslinking after printing)	Adamantine-modified HA (Ad-HA) + β-cyclodextrin-modified HA (CD-HA) (+added methacrylates)	A 3D printer (X-Truder extruder and Revolution XL printer from Quintessential Universal Building Device, Inc.)	Printing speed: 5, 20 and 40 mm/s, Needle gauge: 23, 25 and 27 G, Extrusion rate: 8, 24 and 72 μl/s	Gel-in-gel printing: Spiral structures, multiple inks and structures (spirals and filaments) in the same support, Secondary stabilized: Freestanding pyramidal 3D-structures (ink stabilized) or channels (support gel stabilized)	MSCs and 3T3 fibroblast: >90%, printing process was not affected by the inclusion of cells	[47]
Guest–host(+UV-photocrosslinking after printing)	Adamantine-modified HA (Ad-HA) + β-cyclodextrin-modified HA (CD-HA) (+added methacrylates)	A 3D printer (Makerbot Replicator 2)	N/A	Gel-in-gel printing: a continuous spiral around another one, as well as channels in support	MSCs and 3T3 fibroblasts: high viability	[100]
Guest–host(+UV-photocrosslinking after printing)	Adamantine-modified HA (Ad-HA) + β-cyclodextrin-modified HA (CD-HA) (+added methacrylates, + RGD-functionalization)	A commercial 3D FDM printer (Revolution XL, Quintessential Universal Building Device)	Extrusion flux: 0.33 mL/h, Moving speed: 1.5 mm/s, filament gaps: 1 mm, Needle gauge: 25 G, Temperature: rt	Filaments with greater than 16 layers, depending on the printing parameters (extrusion flux, needle size, speed), the structures remained stable over a month with filament size ranging from 100 to 500 μm (increased extrusion flux resulted increased filament size, whereas increased gauge sized needle and increased needle speed resulted smaller filaments)	3T3 fibroblasts: cells attached to the surface of the printed constructs, scaffolds supported cell adhesion, with cells extending projections and spreading across filaments	[101]
Guest–host(+thiol-ene click chemistry)	Adamantine-modified HA (Ad-HA) + β-cyclodextrin-modified HA (CD-HA) (+norbornene (AdNor-HA) to introduce RGD peptides)	N/A	Needle gauge: 30 G, Extrusion pressure:172 kPa, Speed: 25 and 30 mm/min	Complex microchannels (a range of printed configurations, e.g. straight, stenosis, spiral)	HUVECs: adhere to the printed microchannels and form confluent monolayers across a range of printed configurations. When exposing the cells to angiogenic factors, they degraded the hydrogel with proteases and formed sprouts into the hydrogel, curvature of the microchannel regulated the sprouting	[49]
Guest–host(+UV-photocrosslinking after printing)	Gelatin methacryloyl (GelMA) + a guest–host supramolecule HGSM (isocyanatoethyl acrylate-modified β-cyclodextrin (β-CD-AOI$_2$) + acryloylated tetra-ethylene glycol-modified adamantane (A-TEG-Ad))	A 3D-Bioplotter TM (EnvisionTEC GmbH, Germany)	Needle gauge: 22 G, Disopensing pressure: 8 x 10^4 Pa, Plotting speed: 18 mm/s, Platform temperature: 5°C	Uniform fibers with slightly larger diameter (about 500 μm) compared with setting size (400 μm) due to swelling. The whole construct had homogeneous porous structure.	mBMSCs: high viability (12 days), scaffolds provide favorable microenvironments for cell encapsulation, adhesion and proliferation	[102]
Metal-ion-chelating ligand dynamic coordination bonding (+UV-photocrosslinking after printing)	Bisphosphonate (BP)-functionalized HA + fluorescently labeled bioactive Arg-Gly-Asp-Ser-Cys (RGDSC)	Delta Tower' 3D printer modified with a custom-built syringe extruder	N/A	Letters "O" and "T": in air only two to four layers was a maximum, whereas in support bath system a tube-like structure with hundred layers was possible to print	Osteoblast-like (MG63) cells and human adipose derived stem cells (ASC/TERT1): above 88%, and 80 %	[103]
Ionic (+UV-photocrosslinking after printing)	Support gel: dimethyl acrylate poly (ethylene glycol) (PEGDMA) + alginate + thrombin, Printable gel: fibrinogen	An INKREDIBLE 3D Bioprinter (Cellink, Gothenburg, Sweden) with the double needle	Nozzle speeds: 50 to 600 mm/min, Bioink flow rates: 5 to 10 μL/min, Fibrin fibers printed in at densities: 36, 45, 75, 105, 135, and 165 lines/cm^2, Needle diameter: 500 μm	The printed lines had increasing diameters between 50 to 250 μm when flow rate increased and nozzle speed decreased. Fibrinogen bioink: up to 105 lines/cm^2 no big difference in modulus was seen, whereas after 135 lines cm^{-2} the modulus decreased. The modulus	hMSC: around 90 % (spheroids in fibrin) + a chondrogenic-like differentiation	[104]

(*continued on next page*)

Table 2 (*continued*)

Crosslinking type	Hydrogel components	Printer	Printing specifications	Printing results	Cell viability %	Ref.
				of vertical orientation was slightly higher than that of horizontal resulting anisotropic mechanical behavior. A strain-stiffening behavior was also observed with low density constructs.		
Ionic (+UV-photocrosslinking after printing)	Oxidized and methacrylated alginates (OMAs)	A modified Printrbot 3D printer, a commercial extrusion-based 3D bioprinter (Biobot Basic, Advanced Solutions Life Sciences) or a commercial syringe pump-based 3D bioprinter (Bio X™, Cellink)	Printing needle: 22, 25 and 27 G,	Continuous fibers with high resolution, macroscale cuboid shapes with high 92–110 % fidelity, and large-scale structures, like ear, UIC logo, patterned structure, a two-phase cylinder, concentric-ring and a letter with high fidelity, as well as overhang geometries (a bowl, a bridge, and a letter "K") without using supporting devices or materials	hMSCs: high viability after bioprinting and photocrosslinking (cell-laden complicated 3D-tissue structures with high fidelity and resolution), long-term culture enabled by the secondary crosslinking. The initial structure and shape fidelity were maintained well during long-term chondrogenic culture.	[23]
Ionic	Printed gel: RGD-modified alginate + calcium sulphate ($CaSO_4$), Support gel: calcium chloride ($CaCl_2$) containing gelatin slurry (thermoreversible)	A syringe pump (World Precision Instruments) for single-layer scaffolds or a pressure-mediated bioprinter (Allevi) for expansion lattices	Rate: 200 mL/min (single-layer scaffolds), Needle gauge: 22 G, Temperature: rt	Multilayered alginate lattice printed in support bath, and alternating "S"-shaped layers at a 90^o angle to the layer below extruded with 10 mm side height of 4 layers and 400 μm filament diameter	NPCs: bioink shields NPCs from mechanical damage due to printing. In expansion lattices, NPCs kept the stem-like state while undergoing 2.5-fold expansion	[105]

and in the support, which is beneficial for multicellular structure design. This could also be used for studying cellular behavior within different 3D topographies extruded into hydrogels. It is known that the mechanical strength of these reversible physically crosslinked HA-based hydrogels is inherently low, so they need improvement. Therefore, secondary covalent UV-crosslinking after printing by introducing methacrylates in Ad-HA and CD-HA derivatives was used for stabilization in order to make more complex structures. For example, channels were introduced by removing the unstabilized hydrogels using applied pressure while the support hydrogel is stabilized. [100] Ouyang et al. [101] also previously studied similar dual-crosslinked HA-based hydrogel systems. Secondary photocrosslinking was used to enhance the structural integrity and stability of multilayer structures. Ouyang et al. especially characterized the filaments and 3D-printed structures. A structure formed of filaments with more than 16 layers was able to print. Depending on the printing parameters (extrusion flux, needle size, speed), the structures remained stable over a month with filament size ranging from 100 to 500 μm. For instance, when the extrusion flux increased, the filament size also increased, whereas using a larger gauge needle and increased needle speed resulted in smaller filaments. The peptide-functionalized printed structures supported cell adhesion, such as the attachment of 3T3 fibroblasts on the printed construct's surface and spreading across the filaments. [101] In a more recent study, Song et al. [49] investigated 3D-printing of similar HA-based guest–host systems intended for biomedical applications requiring vessel patterning. The same gel-base was used as ink and support, although the support (Ad-HA component) was further modified with norbornene (AdNor-HA) to introduce RGD peptides for adhesion and permit covalent crosslinking with di-thiol crosslinkers (thiol-ene click chemistry) for stabilization (ink washed away). Complex microchannels were produced allowing integrin-mediated cell adhesion and on-demand protease-sensitive degradation. Human umbilical vein endothelial cells (HUVECs) could adhere to the printed microchannels and form confluent monolayers across a range of printed configurations (e.g., straight, stenosis, spiral). When exposing the cells to angiogenic factors, they degraded the hydrogel with proteases and formed sprouts into the hydrogel. Also, the curvature of the microchannel was shown to regulate the sprouting. [49]

In order to enhance the mechanical strength and self-healing of 3D-bioprintable hydrogels, Wang et al. [102] developed dual-crosslinked 3D-printable hydrogels composed of gelatin methacryloyl (GelMA) and a guest–host supramolecule HGSM (isocyanatoethyl acrylate-modified β-cyclodextrin (β-CD-AOI$_2$) and acryloylated tetra-ethylene glycol-modified adamantane (A-TEG-Ad)). In addition to guest–host crosslinking, UV-crosslinking was used to to improve the stability and accuracy of the 3D-printed structure. The printed fibers were uniform and had a slightly larger diameter (about 500 μm) compared with the setting size (400 μm) due to swelling. The whole construct had a homogeneous porous structure. The compression modulus of these hydrogels reached the level of most human soft tissues. High viability of mBMSCs in 3D-printed fibers after 12 days was also observed. Additionally, good histocompatibility of the constructs was shown by placing them into pockets at the backs of nude mice and keeping them there for 40 days, after which complete integration with autogenous tissue was observed and new muscle tissue and blood vessels formed. [102]

Guest–host crosslinking, used for embedding printing, has, however, some drawbacks, such as the need for a high degree of functionalization or the use of unfriendly organic solvents for modification of polymer. Therefore, Shi et al. [103] introduced a new alternative crosslinking method to overcome these limitations, i.e., metal-ion-chelating ligand dynamic coordination bonding. The ink and support had the same reversible coordination bonding between bisphosphonate (BP) ligands attached to HA backbone and free Ca^{2+} ions. In addition, a fluorescently labeled bioactive Arg-Gly-Asp-Ser-Cys (RGDSC) cell adhesive peptide was attached at defined spatial locations in the construct. A two-step printing-then-stabilization biofabrication using additional

Table 3
Supramolecular self-healing hydrogels for extrusion-based bioprinting. (2/2).

Crosslinking type	Hydrogel components	Printer	Printing specifications	Printing results	Cell viability %	Ref.
Hydrogen bonding (+UV-photocrosslinking)	PEDOT + chondroitin sulfate methacrylate (CSMA) + tannic acid (TA)) + gelatin/ polyethylene glycol	A microextrusion-based 3D printer (GeSim, Bioscaffold 3.2)	Nozzle diameter: 260 μm, Moving speed: 5 mm/s, Pneumatic pressure: 70–90 kPa	The bioink printed into the cell-laden CCH scaffold with a linear filament-based layered-stacking geometry (high shape fidelity and physicochemical properties (i.e. electric conductivity and soft mechanics) similar to native spinal cord tissue)	NSCs: Cells encapsulated in the bioprinted scaffold extended their neurites to form superior physical contact with the neighboring cells as well as the electroconductive matrix, and maintained a predominant *in vivo* neuronal differentiation, accompanying with few astrocytic production in the lesion area after transplantation into the SCI sites.	[106]
Ionic + peptide-peptide interactions	Alginate modified with proline-rich peptide-domains (P1) + a recombinant protein (C7) (MITCH).	A BioBots (Philadelphia, PA, USA) 3D bioprinter	Needle gauge: 32 G, Constant pressure: 10 psi, Print speed: 4 mm/s	Gel-phase bioink (dual-stage crosslinking) maintains cell homogeneity, mechanically protects the cells during printing and can be printed in aqueous medium (prevents the dehydration)	NIH 3T3 fibroblasts and hASCs: 97% and 96% (1 h), respectively, homogeneous cell distribution and improved cell viability during extrusion compared to viscous fluid bioinks. Also, patterned cell cocultures showed minimal cell migration between the lines and <90% cell viability (day 7) post-printing.	[107]
Hydrophobic + thermal	Poly(isopropyl glycidyl ether)-block-poly(ethylene glycol)-block-poly (isopropyl glycidyl ether)	A direct-write printer (The pressure supplied using a Nordson fluid dispenser and the stepper motor stage controlled by a Galil controller)	Nozzle diameter: 100 μm	Pillar structures with high aspect ratio and eight stacked layers with no buckling and sagging of the stacked structures. Overall, easy printing with good resolution and structural integrity.	No cell tests	[108]
Hydrogen bonding (zwitterionic) + UV-photocrosslinking	A sulfobetaine methacrylate monomer (N-(3-Sulfopropyl)-N-methacroyloxyethyl- N,N-dimethylammonium betaine (SPE)) + a nanoclay hydrogel	A multi-process additive manufacturing kit (System 30 M, Hyrel3D, Norcross, GA, USA), equipped with a dispensing module (SDS-5, Hyrel3D, Norcross, GA, USA)	Needle diameter: 250 μm, Speed: 5 to 20 mm/s, a constant positive displacement value: 90 pulses/ microlitre	The tensile properties (strain at break especially) were affected by the printing speed and aging time, whereas compression properties were not so affected. Curing during printing improved the mechanical properties. The printing speed did not have effect if post-curing was used.	Cytotoxicity tests conducted in previous study [109]	[110]
Ionic	Hyaluronic acid (HA) + chitosan (CHI)	A INKREDIBLE + Cellink bioprinter	Printing pressure: 25–45 kPa, Nozzle diameter: 22 and 25 G, Speed: 300, 600 and 800 mm/min	As printing speed decreased, the expansion ratio and uniformity factor (best precision at lower speeds, factor close to 1) increased. The expansion ratio increased with increasing extrusion pressure. Also, 4 layered different shapes (lines, squared zigzag and squared grid) could be printed.	Mouse embryonic fibroblasts (MEFs): about 84% (24 h), the effect of printing was not tested	[111]
Thiol-ene/ thermal/ photocrosslinking/ guest–host	Thiol-ene cross-linked norbornene-modified hyaluronic acid (NorHA), photo-crosslinked poly(ethylene glycol) diacrylate (PEGDA), or thermo-sensitive agarose, and guest–host-based HA-hydrogel as support gel	A modified Revolution XL printer (Quintessential Universal Building Device, Inc.)	Needle gauge: 25G, Printing speed: 20 and 10 mm/min	Traditional layer-by-layer method: ability to print vertical filaments with cross-sectional diameter about 600–700 μm, and four layers. The printing speed, extrusion rate and needle gauge affected to filament diameter. A further secondary stabilization using photocrosslinking was needed. Gel-in-gel printing: ability to print mesoscale spiral patterns with <1 mm filament width, and a checkerboard pattern with discrete material pockets or filaments, as well as fabrication of microchannels in support hydrogel.	NIH 3T3 fibroblast: about 70%, the jamming or the printing process not affecting to viability (about the same before and after printing)	[36]

(*continued on next page*)

Table 3 (*continued*)

Crosslinking type	Hydrogel components	Printer	Printing specifications	Printing results	Cell viability %	Ref.
Ionic + enzymatic	Gelatin-alginate microgels (both as bioink and as suspension medium)	A commercial 3D bioprinter (SunP Inc., China)	3D direct printing: Printing speed: 5 mm/s, Extrusion rate:1.8 μL/s, Temperature: 22 °C. Embedded 3D printing,: Printing speed: 3 mm/s, Extrusion rate:0.38 μL/s, Temperature: 25 °C. SPIRIT printing: 1) first printing of MB bioink: Printing speed: 3 mm/s, Extrusion rate: 0.38 μL/s, Temperature: 25 °C, 2) second printing of gelatin bioink: Printing speed: 3 mm/s, Extrusion rate: 0.76 μL/s, Temperature: 24 °C	(1) printing of bioink in a reversible suspension medium to generate the complex external geometry of organ/tissue, and then (2) printing of sacrificial ink into the freshly printed construct (uncrosslinked) to generate a freeform vascular network, (3) followed by in situ photo-crosslinking, and removal of (4) suspension medium and (5) sacrificial ink.	hiPSCs: 45.8% (after printing and crosslinking), ability to print a ventricle model with perfusable freeform vascular network.	[82]

photopolymerization (acrylamide-functionalized HA-BP) was also applied. The printability was tested by extruding letters "O" and "T"; in air, only two to four layers were a maximum, whereas in the support bath system, a tube-like structure with a hundred layers was possible to print. The printed construct was then photocrosslinked and isolated from unstabilized support bath by cleaving the BP·Ca^{2+} coordination bonds in an acidic environment, leaving a printed construct with no visual change. The viability of 3D-encapsulated osteoblast-like (MG63) cells and human adipose-derived stem cells (ASC/TERT1) was above 88%, and 80 %, respectively, in physically, chemically, and dually crosslinked hydrogels. [103] de Melo et al. [104] (Fig. 6 (b)) also used the previously described embedding bioprinting method since it enables the material to be soft at the microlevel, which stimulates encapsulated cells, whereas at the macroscopic tissue level, it is orders of magnitude stiffer. They developed a cartilage-like tissue construct by using a support bath consisting of a self-healing interpenetrating polymer network (IPN) hydrogel composed of a light-induced covalently crosslinked dimethyl acrylate poly (ethylene glycol) (PEG) and a cation-induced physically crosslinked alginate prepolymer mixture. This mixture, by being stiff and having tough mechanical properties, can withstand cyclic loads and high mechanical stresses, while a printable ink consisting of fibrinogen and thrombin (fibrin hydrogel) provides a soft and stimulative environment for cells to maintain chondrogenic function. Alone, printing of fibrinogen using traditional extrusion printing is difficult. The physical supramolecular interactions between the two polymers provide the self-healing property to the support bath, whereas non-crosslinked alginate provides the shear-thinning behavior. After printing, secondary photocrosslinking was used for the support bath. hMSC spheroid-laden bioink was extruded in the support bath without any visual cracks seen in support. The bioprinted spheroids in fibrin showed higher viability (around 90 %) compared with spheroids in bulk PEG-alginate (around 80 %). A chondrogenic-like differentiation was also shown to be favored. The printability was tested by examining how printed fiber diameter was affected by varying nozzle speeds (50 to 600 mm/min) and bioink flow rates (5 to 10 μL/min). Needle diameter was kept constant (500 μm). The printed lines had increasing diameters between 50 to 250 μm when the flow rate increased and the nozzle speed decreased. Additionally, fibrinogen bioink was printed in different densities (36, 45, 75, 105, 135, and 165 lines cm^{-2}) and orientations (vertical and horizontal) to study the effect of fibrin patterns on IPN hydrogel mechanical properties. Up to 105 lines cm^{-2}, no big difference in modulus was seen, whereas after 135 lines cm^{-2}, the modulus decreased. The modulus of the vertical orientation was slightly higher than that of the horizontal orientation, resulting in anisotropic mechanical behavior characteristic of natural cartilage. A strain-stiffening behavior was also observed with low-density constructs, providing possible self-protective properties against any trauma. [104]

Jeon et al. [23] (Fig. 6 (c)) studied ionically crosslinked oxidized and methacrylated alginates (OMAs) with shear-thinning, low shear yield stress, and rapid self-healing properties to be used also as a bioink for EBB, for example for cartilage TE. Further stabilization was achieved using secondary photocrosslinking. Direct extrusion of OMA bioinks through a printing needle (22, 25 and 27 G) as continuous fibers with high resolution was shown. Also, printing of macroscale cuboid shapes with high 92–110 % fidelity was also shown, as well as printing of large-scale structures, like an ear, UIC logo, patterned structure, a two-phase cylinder, concentric ring, and a letter with high fidelity. In addition, printing of overhang geometries (a bowl, a bridge, and a letter "K") without using supporting devices or materials was also shown for the first time. Bioprinting of hMSCs-laden calcium-crosslinked OMA hydrogels into complicated 3D-tissue structures was also possible with high fidelity and resolution. The cell viability was high after bioprinting and photocrosslinking. 3D-bioprinted construct's long-term culture was enabled by the secondary crosslinking. The initial structure and shape fidelity were maintained well during long-term chondrogenic culture. Using these OMA bioinks, not only are the fidelity, resolution, and

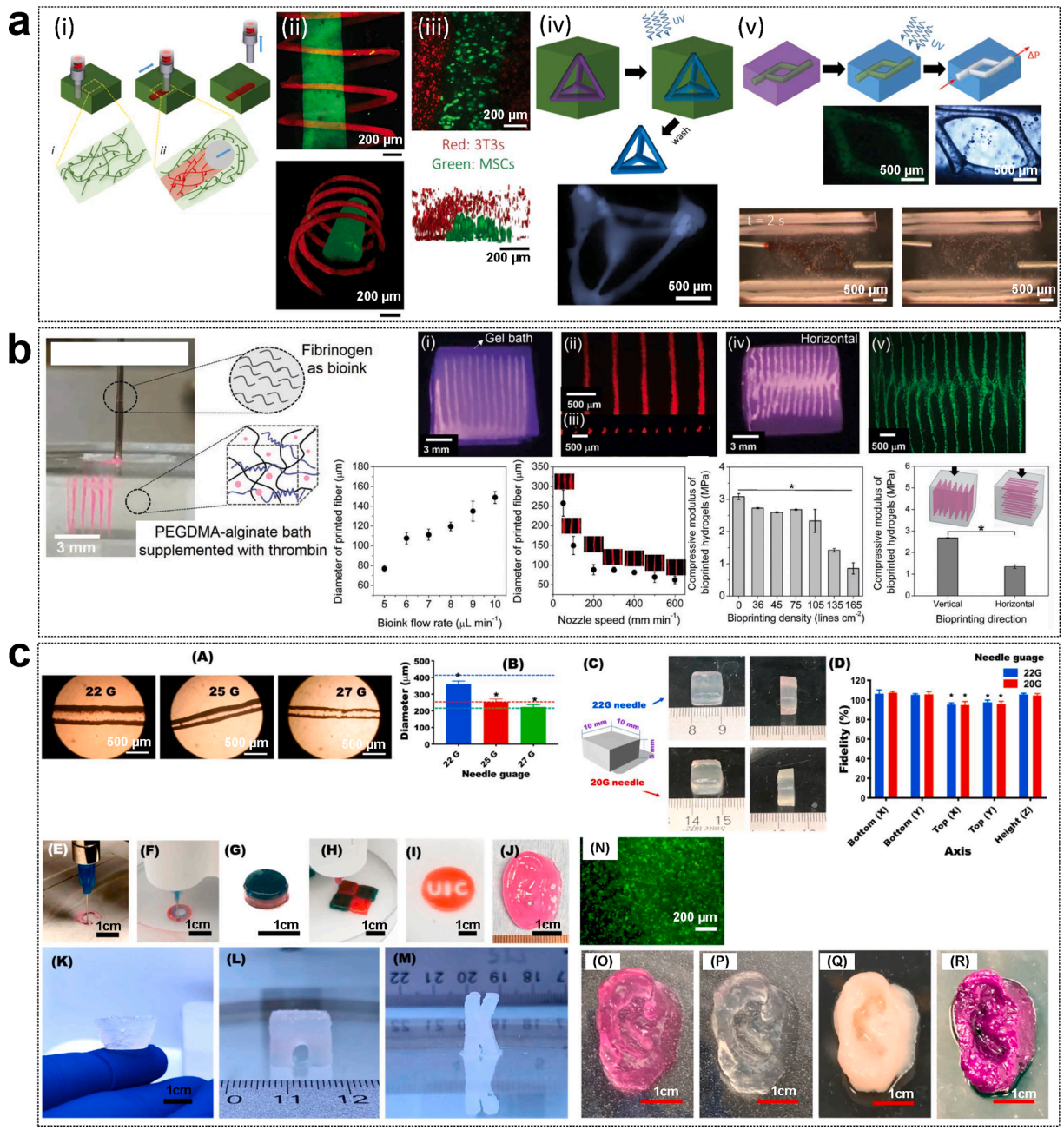

Fig. 6. Extrusion-based bioprinting of supramolecular hydrogels. (a) i) Extrusion of supramolecular ink (red) into supramolecular support gel (green) (both composed of guest–host-crosslinked HA-based hydrogels), ii) a continuous spiral (rhodamine-labeled ink) and a filament (fluorescein-labeled ink) printed into support gel (unlabeled), iii) bioink containing MSCs (green) printed into support gel containing 3T3 fibroblasts (red), and iv) printing of self-supporting pyramidal structures (ink stabilized) and v) channels (support gel stabilized) [47]. (b) 3D-printing of fibrinogen bioink into bath composed of PEG-alginate supplemented with thrombin, printed fibrin fiber diameters as a function of flow rate and with respect to nozzle speed, and compressive modulus of bioprinted IPN hydrogels with different bioprinting densities (lines cm^{-2}) and direction of lines (vertical or horizontal, 105 lines cm^{-2}) [104]. (c) A) 3D-printed filaments composed of ionically-crosslinked OMA hydrogels using different sized needles and B) their mean diameters (dotted lines indicate inner diameter of printing needle), C) 3D-printed structures using 22 and 20 G needles and D) their printing fidelities, E-J) different 3D-printed structures (letter "C", concentric ring, two-phase cylinder, checkerboard-patterned structure, UIC logo and ear), and K-M) 3D-printed overhanging geometries (bowl, bridge and letter "K"). N) Live/dead staining of hMSCs in photocrosslinked 3D-printed OMA constructs (day 0), and 3D-printed hMSC-laden OMA ears O) before, or P) after photocrosslinking, and chondrogenic differentiated ears Q) before or R) after Toluide blue O staining. [23] Reprinted with permission from Highley et al. (2015) [47] Copyright ©2015 Wiley Online Library, de Melo et al. (2019) [104] Copyright ©2019 Wiley Online Library, and Jeon et al. [23] Copyright ©2022 Elsevier.

mechanical stability problems addressed, but also the independent control of their cell adhesivity, swelling, degradation and mechanical properties, as well as the capacity to deliver bioactive molecules is possible. [23]

In case of bioinks for neural TE applications, Lindsay et al. [105] studied RGD-modified alginate electrostatically crosslinked with calcium sulphate ($CaSO_4$) (first-stage crosslinking with low cation concentration and second-stage with high cation concentration) to be used as bioink for neural progenitor cells (NPCs) expansion lattices. Due to reversible nature of electrostatic bonds, these hydrogels have stress relaxation property and encapsulated cells can remodel them. First-stage crosslinking forms extrudable and weak shear-thinning and rapidly self-

healable gel before printing, preventing cell sedimentation and protecting cells during printing, whereas second-stage crosslinking forms stiffer, remodelable material post-printing that supports different cell functions. The multilayered alginate lattice was printed in calcium chloride ($CaCl_2$) containing gelatin slurry support bath, after which the support was replaced with Stemness Maintenance Medium supplemented with $CaCl_2$. Alternating "S"-shaped layers at a 90^o angle to the layer below were able to extrude with 10 mm side height of 4 layers and 400 μm filament diameter. This alginate bioink was also shown to shield NPCs from mechanical damage due to printing. In expansion lattices, NPCs kept the stem-like state while undergoing 2.5-fold expansion. [105] In more recent study, since it is known that uncontrollable differentiation of neural stem cells (NSCs) in the host can lead to a poor therapeutic effect in nerve tissue repair, Song et al. [106] developed a new approach to precisely construct TE scaffolds for stem cell-based therapy for traumatic spinal cord injury. They fabricated a shear-thinning self-healing composite bioink consisting of a novel conductive polymer (poly(3,4-ethylenedioxythiophene) (PEDOT):chondroitin sulfate methacrylate (CSMA):tannic acid (TA)) that was integrated into a photocrosslinkable gelatin/ polyethylene glycol physical-gel matrix. The bioink was printed into the NSC-laden conductive composite hydrogel (CCH) scaffold with a linear filament-based layered-stacking geometry, which had high shape fidelity and physicochemical properties (i.e., electric conductivity and soft mechanics) similar to native spinal cord tissue. Physical contact for the NSCs with adjacent cells and surrounding matrix was improved, as well as the *in vivo* astrocytic production for the NSC-laden conductive composite scaffold was significantly inhibited. The removal of glial scar tissues and the regeneration of well-developed nerve fibres sequentially happened, which not only facilitated nerve tissue development but also accelerated locomotor function recovery in the spinal cord injury (SCI) rats. Thus, this material was shown to be promising for NSC delivery in SCI therapy. [106]

As printing continues, there might be problems like printer clogging or inhomogeneous distributions in the construct due to cell sedimentation in viscous fluids, cell death due to the shear forces experienced by the cells, or dehydration of the encapsulated cells due to printing in the air. Dubbin et al. [107] presented a new self-healing two-component extrudable bioink consisting of alginate modified with proline-rich peptide-domains (P1) and a recombinant protein (C7) that form a weak physical network (also referred to as a mixing-induced two-component hydrogel, MITCH). During printing, the bonds between the peptide-peptide domains are disrupted, resulting in shear-thinning, making the extrusion of bioink easy. Dual-stage crosslinking is done by directly printing the shear-thinning gel in a calcium bath. This gel-phase bioink having dual-stage crosslinking can maintain cell homogeneity, mechanically protects the cells during printing, and can be printed in an aqueous medium which prevents dehydration. The cytocompatibility of these gels was tested with NIH 3T3 fibroblasts and human adipose-derived stem cells (hASCs) which both showed high viability (97% and 96%, respectively), homogeneous cell distribution, and improved cell viability during extrusion compared to viscous fluid bioinks. Also, patterned cell cocultures, i.e., parallel lines alternating between cells, or cells patterned into overlapping perpendicular lines, were printed that showed minimal cell migration between the lines and high cell viability (<90%) post-printing. [107]

F127-based hydrogels are commercially available inks that have been mainly used as sacrificial materials for 3D-printing. Their limitations in properties such as modulus or yield stress do not enable printing of more complex 3D-structures. Therefore, Zhang et al. [108] developed, similar to F127, dual stimuli-responsive (shear force and temperature) supramolecular hydrogels comprised of poly(isopropyl glycidyl ether)-block-poly(ethylene glycol)-block-poly(isopropyl glycidyl ether) to be used as a bioink in extrusion-based direct-write printing into 3D-constructs. The thermoreversible nature of these hydrogels is helping the loading of ink into the printer's syringe. This dynamic ink was shown to have rapid and reversible modulus response to shear stress (shear-thinning). In addition to shear-thinning behavior, the yield stress was studied. Yield stress showed to be higher leading to better printing quality compared, for example, with similarly behaving F127 gels. The printing of pillar structures with high aspect ratio and eight stacked layers was proved possible. No buckling and sagging of the stacked structures were shown. Overall, the printing of structures was easy with good resolution and structural integrity. However, no cell tests were performed. [108]

Sällström et al. [110] produced a nanoclay-crosslinked zwitterionic sulfobetaine hydrogel to be 3D-printed either using curing during printing or a printing-then-curing approach. The nanoclay gives shear-thinning properties and works as an internal support making possible this extrusion-based printing without external support. The effect of different printing speeds (5–20 mm/s) on mechanical properties of printed structures was tested. The tensile properties (strain at break especially) were affected by the printing speed and aging time, whereas compression properties were not so affected. However, in compression hysteresis test aging affected the material's recovering ability and dissipated energy. Curing during printing improved the mechanical properties. The printing speed did not have effect if post-curing was used. These hydrogels showed self-healing abilities and recovered from compression at room temperature. In addition to showed properties, the cell tests conducted in their previous study also supported the use of these hydrogels for bioprinting of TE scaffolds. [110]

Maiz-Fern*a* ndez et al. [111] studied the potential use of self-healing HA/chitosan(CHI) polyelectrolyte complex hydrogels in extrusion-based 3D-printing. For optimization of the suitable printing concentration of polysaccharides solutions, contact angles were measured to evaluate the spreadability of the solutions. The printability was evaluated by studying the effect of printing pressure (25–45 kPa), diameter of the nozzle (22 and 25 G), speed (300, 600 and 800 mm/min), and printing surface (glass, polystyrene, Teflon and metal) on the printed hydrogels. Also, the expansion ratio and uniformity factor were determined. The results showed that when printing speed was decreased, the expansion ratio and uniformity factor (best precision at lower speeds, factor close to 1) increased. The expansion ratio also increased with increasing extrusion pressure. Also, 4 layered different shapes (lines, squared zigzag, and squared grid) could be printed. The viability of mouse embryonic fibroblasts (MEFs) in HA/CHI hydrogel was about 84% after 24 h, although the effect of printing was not tested. [111]

Highley et al. [36] (Fig. 7 (a)) introduced an alternative way to make inks by using jammed microgels having shear-thinning and self-healing properties that permit the flow and recover rapidly after deposition. The pre-crosslinked microparticles were immobilized through physical interactions with surrounding particles. These inks could be deposited either on the surface or in a support bath, and further secondary stabilized. Their properties were based on the microgel itself but also on their mix. The behavior of jammed microgels was solid-like until the application of a certain amount of force induced movement of microgels relative to one another. Below the yield stress when applied stress was reduced, the system recovered again. Highley et al. introduced three types of microgels: norbornene-modified hyaluronic acid (NorHA) and poly(ethylene glycol) diacrylate (PEGDA) either crosslinked by using radical chain-growth polymerization or thiol-ene photoinitiated crosslinking, and thermally crosslinked (by cooling) agarose. Traditional layer-by-layer extrusion on a surface and gel-in-gel printing (guest–host-based HA-hydrogel as support gel) were tested with all gel types (NorHA, PEGDA or NorHA + PEGDA). With the traditional layer-by-layer method, vertical filaments with a cross-sectional diameter of about 600–700 μm were printed. Also, four layers were able to be printed, and printing speed, extrusion rate, and needle gauge were shown to affect filament diameter. Further secondary stabilization using photocrosslinking was needed. In gel-in-gel printing, mesoscale spiral patterns with <1 mm filament width were extruded. In addition, a checkerboard pattern with discrete material pockets or filaments could

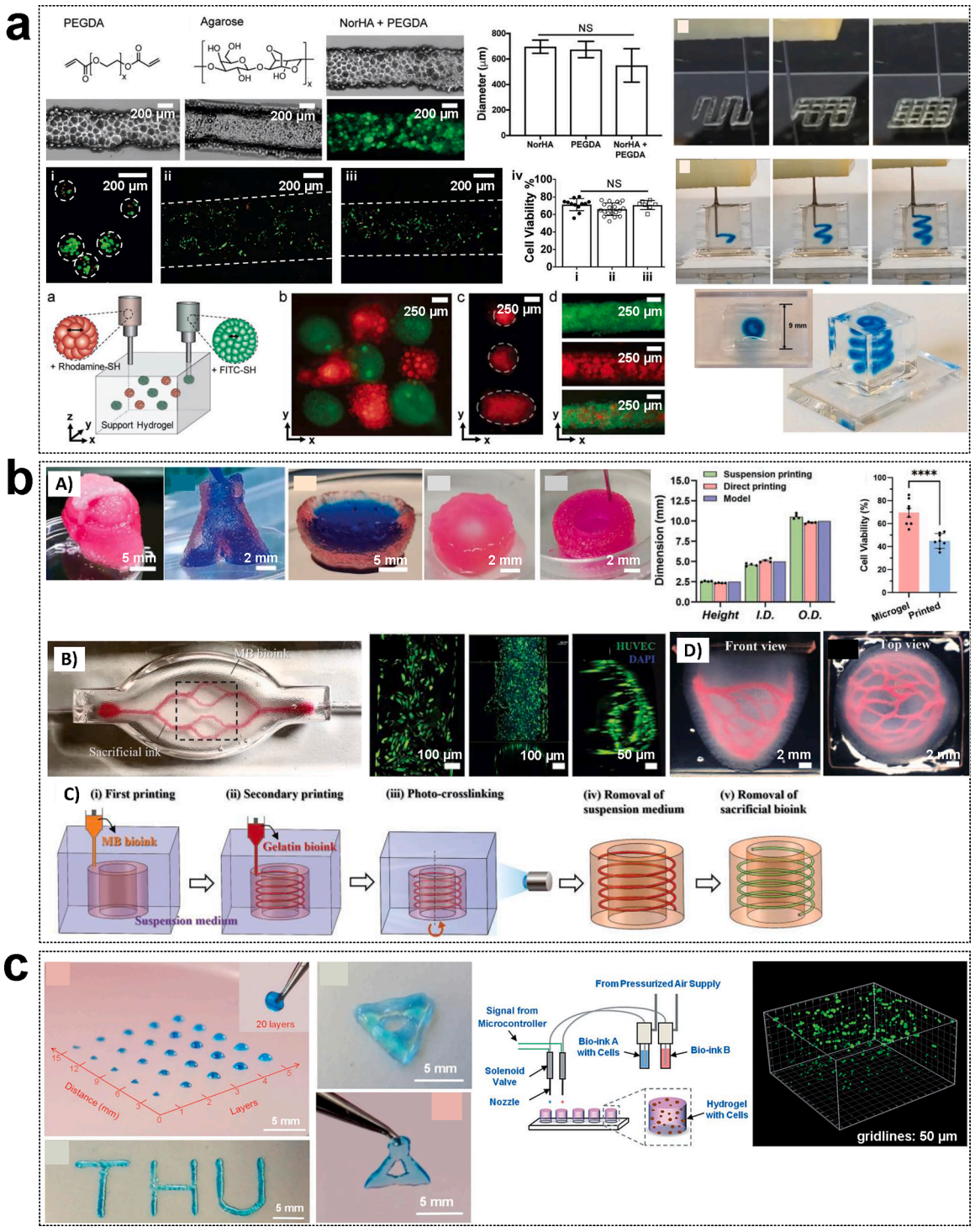

Fig. 7. Extrusion- and inkjet-based bioprinting of supramolecular hydrogels. Extrusion-based bioprinting (a) of jammed microgels: extruded PEGDA, agarose and NorHA + PEGDA microgel inks and their filament diameters, printing of microgel inks onto glass surface (lattice structure) or as spiral structures (blue) within shear-thinning support gel, live/dead staining of 3T3 fibroblasts within microgels (i) after fabrication, (ii) after jamming & extrusion onto a surface, and (iii) within shear-thinning hydrogel, and (iv) cell viability (%) in these conditions, and a) printing of jammed NorHA microgel inks within shear-thinning hydrogel support, (b) an array of ink depots, (c) depots of different sizes and (d) straight lines of mixed or individual microgel inks [36]. (b) (A) Embedded 3D-bioprinting of MB bioink: heart model after removing from suspension medium, open chamber containing blue ink (no leakage), tubular structures by embedded printing (after exacting from the Carbopol-based suspension medium) and direct printing, respectively, and their measured heights, and viability of hepatic cells within GelMA and MB bioinks, respectively. B) Embedded printing of a branched vascular structures within the MB bioink-based suspension medium, green fluorescent-labeled HUVEC adhesion and spreading on the channel wall (day 3), HUVEC endothelium monolayer formation (day 7), and 3D-reconstructed microvessel formed by endothelial cell self-assembly. (C) SPIRIT printing containing 5 printing processes. D) Optical images showing 3D-printed vetricle with densely packed vascular network at the front and top, respectively, fabricated by SPIRIT. [82] (c) Inkjet-based bioprinting of supramolecular polypeptide-DNA hydrogels: the distance of printed droplets with increasing number of layers, printed letters ("THU", 5 layers) and a triangle (ten layers, able to pick up by tweezers), cell-printing process using inkjet technique, and 3D-stack of AtT-20 cells inside hydrogel (FDA staining in green) [34]. Reprinted with permission from Highley et al. (2019) [36] Copyright ©2019 Wiley Online Library, Fang et al. (2023) [82]Copyright©2023Wiley Online Library, and Li et al. (2015) [34] Copyright ©2015 Wiley. Online Library.

be printed, as well as fabrication of microchannels in the support hydrogel. The jamming or the printing process was also shown not to affect NIH 3T3 fibroblast viability (viability about 70%), which was about the same before and after printing. The individual microgels with elastic and flow properties together protect the cells from shear stresses during printing. Overall, Highley et al. stated that when using supports, the internal forces should be resisted by the inks since they can be either broken into droplets or the print nozzle can drag them. Also, the external forces from support (like dynamic rearrangements) should be resisted since those can lead to compression and cause flowing of the deposited inks. [36]

Fang et al. [82] also studied microgel-based bioinks (Fig. 7 (b)). The replication of the external geometry of specific organs and their internal structure (i.e., blood vessels) simultaneously has been a challenge. Thus, Fang et al. developed a bioprinting strategy called sequential printing in a reversible ink template (SPIRIT), in which a shear-thinning self-healing microgel-based biphasic (MB, gelatin-alginate microgels double crosslinked with ionic and enzymatic crosslinking) bioink was used both as a bioink and as a suspension medium supporting embedded 3D-bioprinting. In SPIRIT, there were several stages, i.e., (1) printing of bioink in a reversible suspension medium to generate the complex external geometry of organ/tissue, and then (2) printing of sacrificial ink into the freshly printed construct (uncrosslinked) to generate a freeform vascular network, (3) followed by *in situ* photo-crosslinking, and removal of (4) suspension medium, and (5) sacrificial ink. When encapsulating human-induced pluripotent stem cells (hiPSCs) in these MB bioinks, 45.8% cell viability after printing and crosslinking was achieved. Fang et al. also were able to print a ventricle model with perfusable freeform vascular network. [82]

3.3. Supramolecular self-healing hydrogels for inkjet- and stereolithography-based bioprinting

This section presents supramolecular self-healing hydrogels for inkjet- and stereolithography-based bioprinting. All the presented hydrogels are also collected in Table 4.

Li et al. [34] (Fig. 7 (c)) introduced for the first time a supramolecular polypeptide-deoxyribonucleic acid (DNA) hydrogel to be used as a bioink for *in situ* multilayer 3D-bioprinting using inkjet-based printing for TE. The gel composed of two components, a polypeptide-DNA conjugate (bio-ink A) and a complementary DNA linker (bio-ink B), and formed rapidly (within seconds). The dynamic nature was based on the DNA hybridization. The printing of hydrogel droplets (20 layers) and different shapes (i.e., letters "THU" and triangle of 10 layers) were tested. The high mechanical strength and healing properties enabled the printing of geometrically uniform structures without boundaries and the keeping of the millimeter scale shapes without collapsing. In addition, no shape deformations of printed droplets after printing due to shrinking or swelling were shown. Further, the printed AtT-20 cells (an anterior pituitary cell line) maintained viability (98.8 %) and functionality. Also, cultures of two types of cells (AtT-20 and HEK-293 cells (human embryonic kidney (HEK) 293 cell line)) showed high viability of cells. DNA hydrogels were also biodegradable, permeable, and had designed responsiveness (e.g., temperature, pH, light, etc.). All the above properties overcome many limitations of non-covalently crosslinked natural-based hydrogels and covalently crosslinked hydrogels used for 3D-printing [34].

Another example is a stereolithography-based study of Chen et al. [35], where self-healing hydrogels crosslinked with hydrophobic association by copolymerizing ampholytic cross-linker (2-(di-methylamino) ethyl methacrylate and methacrylic acid) with butyl acrylate followed by soaking in water were prepared. An ampholytic crosslinker that can induce hydrophobic association by hydrating with water can be used to replace, for example, covalent crosslinkers that have weaker self-healing efficiency. These hydrogels showed high healing efficiencies (up to 100%, tensile strength) and stretchability (elongation above 1000%). The crosslinker supported the 3D-printing fabrication of a hydrogel precursor when using a stereolithographic 3D-printing system, i.e., an auricular precursor was printed followed by a UV light-emitting diode (UV-LED) irradiation for enhanced polymerization efficiency and soaking in water to result in a hydrogel possessing a sound appearance of the human ear. These hydrogels also showed low cytotoxicity (viability after 48 h and 72 h above 90% and 85%, respectively) when tested with L929 mouse fibroblast cells. [35]

4. The current status and future of self-healing hydrogels and bioinks made from them

Self-healing hydrogels, designed to overcome limitations of traditional counterparts, offer a versatile solution for tissue engineering, particularly in the realm of 3D-bioprinting. Their unique properties address issues such as poor mechanical strength and facilitate improved stability and durability. This section explores the advantages of dynamic hydrogel-based bioinks at various stages of 3D-bioprinting. However, these promising bioinks also face challenges that should be taken into account when designing them. Looking ahead, the future of 3D-bioprinting involves, for example, patient-specific, multifunctional tissue grafts, complex tissues with vascularization, and the incorporation of

Table 4
Supramolecular self-healing hydrogels for inkjet- and stereolithography-based bioprinting.

Crosslinking type	Hydrogel components	Printer	Printing specifications	Printing results	Cell viability %	Ref.
DNA hybridization	A polypeptide-DNA conjugate (bio-ink A) + a complementary DNA linker (bio-ink B)	A Heriot-Watt University's valve-based bioprinter	N/A	Ability to print hydrogel droplets (20 layers) and different shapes (i.e. letters "THU" and triangle of 10 layers), geometrically uniform structures without boundaries, keeping of the millimeter scale shapes without collapsing, no shape deformations of printed droplets after printing due to shrinking or swelling. The smallest printed droplet: diameter: approx. 500 μm, thickness: 80 μm, volume: 60 nL.	AtT-20 cells: 98.8 %, Cultures of two types of cells: 99.1 % for AtT-20 cells (48 h), and 99.3 % (48 h) and 95.8 % (96 h) for HEK-293 cells	[34]
Hydrophobic	(2-(di-methylamino) ethyl methacrylate and methacrylic acid) + butyl acrylate	A desktop stereolithographic 3D printer with a liquid crystal device (Anet N4, Shenzhen Anet Technology Co., Ltd, Shenzhen, China)	Platform moving speed:3 mm/s, Curing time: 90 s. After the printing: the hydrogel precursors were further irradiated under a UV-LED (365 nm) for another 1 h.	Ability to print "human ear"	L929 mouse fibroblast cells: above 90% (48 h) and 85% (72 h)	[35]

Table 5
Advantages, design considerations and characterization of self-healing hydrogel-based bioinks and bioprinted constructs, and future trends in 3D-biopinting.

Aspect	Considerations
Advantages of self-healing hydrogel-based bioinks	
1. Prior to bioprinting	• Prevention of cell sedimentation due to viscoelastic nature. [52,10]
2. During bioprinting	• Reduction of shear stresses during bioprinting. [52,10,113]
3. During solidification	• Rapid self-healing capability for structural integrity and shape fidelity after printing. [52,10]
	• Interlayer adhesion improvement due to rapid healability. [52]
4. Post-printing maturation	• Enable cellular remodeling and tissue formation. [114,115]
	• Mimic natural tissues' complex rheological properties. [58]
Design considerations of self-healing bioinks	
	•Scalability and ability to hold 3D-shape as long as needed. [52]
	•Tunable network behavior, dynamic timescales, and shear-thinning properties. [52]
	•Time-dependent and robust printing performances, i.e., rapid formation and maturation prior printing, and recovery after printing, shear-thinning properties, and suitable yield stress. [10,42]
	•Hydrogels that can heal on command (due to the highly dynamic and load-bearing nature of the microenvironment of tissues). [24]
	•Designing hydrogels with electrical and mechanical properties that are found in natural tissues. [24]
	•Mechanically tough hydrogels that can quickly self-heal to resist the traction forces by cells. [24]
	•Designing formulation that is both self-healing and mechanically robust. [10]
	•Dynamic double network- or composite-based bioinks as single reversible linkages may have poor mechanical strength and stability. [53,24,116,117]
	• Noting that secondary crosslinking (if used) may limit the self-healing capability. [17,6,52,3]
	•Dynamic bioinks based on reversible covalent crosslinking for improved strength. [10]
	•Optimizing dynamic bioinks' properties for *in vivo* models with stem cells. [5,18]
	•Cyto-protective and biocompatible bioink with tunable release. [5]
	•Incorporating oxygen and nutrient supply to quiescent cells for optimal implant lifetime. [18]
	•Cytocompatibility and stability under physiological conditions of unbound and bound forms. [52]
	•Selective reactivity or unreactivity towards cellular secretions so that dynamic nature is not blocked. [52]
	•Overcoming spatiotemporal evolution of network properties across timescales. [52]
	•Mimicking ECM's hierarchical complexity, e.g., using heterogeneous hydrogel-firm substance-mixtures, or incorporating biochemical and mechanobiological cues. [10,3]
	•Multimaterial bioprinting for complex heterogeneous structures. [3]
	•Multifunctionality in bioinks (for example incorporating therapeutic and diagnostic factors in the same system). [18]
Characterization and modeling of self-healing bioinks and bioprinted constructs	
	•Diverse prior- and post-characterization of bioinks for improved 3D-bioprinted construct design. [3]
	• Extensive characterization of rheological properties of bioinks, e.g., rheology of gelation kinetics prior printing. [10]
	•Exploration of self-healing hydrogel stability in physiological conditions and in vivo conditions. [18]
	•Characterization of self-healing properties of bioinks in depth. [3,51]
	•Computational modeling and real-time monitoring for optimization of 3D-bioprinted construct design. [3]
Future trends in 3D-bioprinting	
	•Fabrication of patient-specific, multifunctional tissue/organ grafts. [7,13,3]
	•Fabrication of complex heterocellular tissues with multi-scale vascularization and innervation, and drug delivery systems. [7,13,3]
	•Using combination of multiple printing techniques for reduced production period and enhanced complexity. [7,13]
	•Achieving functional constructs with heterogeneity, gradients, complexity, and anisotropy. [7,13]
	•Ability to apply external fields during printing if inclusion of functional nanoparticles is needed. [7,13]
	•Transitioning more from 3D-bioprinting to 4D-bioprinting to imitate dynamic characteristics of complex organs. [118,3,39]

functional nanoparticles. All these aspects and considerations are also summarized in the accompanying Table 5.

Self-healing hydrogels have the general advantages of hydrogels, but they are also designed to overcome challenges related to traditional hydrogels, such as poor mechanical strength or low resistance to wear and tear, in order to improve their stability and durability [18]. Thus, these properties make self-healing hydrogels potential for different TE applications, including 3D-bioprinting. The advantages of using dynamic hydrogel-based bioinks in 3D-bioprinting can be divided in four categories: (1) prior to bioprinting, (2) during bioprinting, (3) during solidification, and (4) post-printing maturation. First, prior to printing, cell sedimentation, that can lead to inhomogeneous cell distribution, can be prevented by using dynamic bioinks due to their viscoelastic nature (not liquid) when in a syringe. Second, dynamically crosslinked hydrogels have a liquid-like state when the links are ruptured by shear forces, which further reduces shear stresses that can decrease cell viability and function [113] during the bioprinting process and thus ease bioprinting. Third, after shear-thinning and network rupture, dynamic bioinks can self-heal, i.e., they can regain structural integrity after printing. The healing should be fast enough so that shape fidelity is not lost. [52,10] However, the extrapolation of rheological self-healing measurements to macroscopic self-healing should be done with caution, since timescales are often different [15]. Interlayer adhesion can also be improved by this rapid healability [52]. Forth, it is known that highly covalently crosslinked hydrogels are not permissive to cellular remodeling or maturation, whereas dynamic hydrogels can enable cellular remodeling [114] and tissue formation [115], but also mimic many natural tissues' complex rheological properties [58].

Self-healing dynamic bioinks, however, are not without challenges. There are some design considerations that should be taken into account when designing these bioinks. Basic requirements such as scalability and ability to hold 3D-shape as long as needed for tissue formation are required. The dynamic hydrogel bioinks should also be designed rationally so that their network behavior, dynamic timescales, and shear-thinning property would be tunable. [52] One major challenge is, however, how to make printable ink with time-dependent and robust printing performances. For example, rapid formation and maturation of gels prior printing are needed [10]. Also, rapid recovery time after disruption is needed in order to minimize material loss, but the ink should also have shear-thinning properties to be able to extrude through a needle, and suitable yield stress (>100 Pa) for material retention and shape fitting [42]. As the microenvironment of tissues is usually highly dynamic and load-bearing, it is also necessary to design hydrogels so that they can heal on command, but also to incorporate some electrical

and mechanical properties that are found in natural tissues [24]. Also, as in a case of cell-encapsulated hydrogels, the structural integrity of hydrogels will eventually be disrupted due to traction forces by cells (due to rapid migration and interface pulling), it is necessary to design mechanically tough hydrogels that can quickly self-heal in order to achieve optimal implant lifetime [24]. It is, however, challenging to find formulation that is both self-healing and mechanically robust (they are usually opposing) [10]. This could be done, for example, by tuning the inks using nanocomposites [119–122], double network systems (e.g., multiple self-assembled systems [123,124], or dynamic/dynamic or dynamic-static combinations [107,101,125]). It is also known that single reversible linkages, regardless of whether they are physical or chemical bonds, on their own may have poor mechanical strength and stability, which is why double networks or composites are also needed [53,24,116,117]. It should be noted, however, that secondary crosslinking can make the system more complicated and even limit the self-healing capability, or in case of photocrosslinking as a secondary crosslinking method, photoinitiators can be cytotoxic and UV-irradiation can cause damage [17,6,52,3]. It is also known that even if covalently crosslinked hydrogels are more challenging to print than physical hydrogels due to their higher viscosity, they have higher stability and diverse functionality. In the future, more dynamic bioinks based on covalent crosslinking should be developed since they can give strength but also can mimic non-covalent linkages' reversible nature. [10]

Only few of the current dynamic bioink hydrogel systems have been used in *in vivo* models where hydrogels encapsulate stem cells [5,18]. Even though it has been shown that encapsulated stem cells can maintain their stemness and enter a state of quiescence, the quantities of cells are still low [18]. Development of these systems is therefore needed; they should maintain shear-thinning and self-healing properties while having high fracture toughness, but also have cyto-protective behavior, tunable release, and biocompatibility [5]. Most importantly, the supply of oxygen and nutrients should be enabled to quiescent cells, and to design these dynamic hydrogels so that they would promote stem cell maturation toward tissue regeneration [18]. In addition, the bioinks' unbound and bound forms should be stable under physiological conditions and cytocompatible, as well as be selectively reactive or unreactive towards cellular secretions when exposed to cells so that their dynamic nature is not blocked [52]. In addition, even though the dynamicity of these hydrogels can provide a permissive dynamic environment for cells, in theory they can also infinitely diffuse, swell, expand, and creep, all depending on timescale. The network properties' spatiotemporal evolution across timescales is one of the most important challenges to overcome in terms of biomimetic materials. [52] In general, in order to obtain well-functioning TE constructs in the future, the improved knowledge and understating of the interactions between the target tissue and self-healing hydrogels would be important.

The next generation of bioink hydrogels should also replicate ECM's hierachical complexicity [10]. Hydrogels can be made heterogeneous mixtures by combining with firm substances (e.g., hydroxyapatite, nanofibrillated cellulose, bioactive glass, dual-crosslinking, etc.) to improve e.g., their mechanical, thermal, or electrical properties [3]. Also, for example, incorporation of biochemical and mechanobiological cues would also be needed to induce certain cellular response [52,3]. Multimaterial bioprinting is therefore needed to achieve these complex heterogeneous structures [3]. Multifunctionality of the self-healing hydrogel-based bioink would also be desired, for example, to have both therapeutic and diagnostic factors in the same system. This could be achieved by combining different nanoparticle systems, or by incorporating multiple release of drugs/agents (each target to different pathways) in the same system (or even have multiple release kinetics for different agents). However, it is important to understand the behavior of dynamic bonds in these varying conditions. [18]

In terms of designing the bioink, the diverse prior- and post-characterization of bioink is crucial so that the final bioprinted construct can be improved. In a review by Karvinen et al. [3], some prior- and post-printing properties of bioinks (for EBB) and their characterization have been presented. Pre-printing characterization of bioink can be divided into viscosity, yield stress, shear performance (shear-thinning property), recovery time (self-healing ability), and shape fidelity. Post-printing characterization of 3D-bioprinted construct, on the other hand, can contain optical image analysis (bioinks' post-crosslinking printability, spreading, and quality), compressive mechanical analysis (construct's compressive modulus and mechanical stability), and degradation and swelling analysis. [3] For example, the rheological properties, crosslinking degrees, and formulation should be accurately controlled to be able to find an ideal printable ink, and therefore the rheology of gelation kinetics should be tested prior printing [10]. Another example is the stability of self-healing hydrogels in physiological conditions, which has not yet been studied in depth. There have already been studies showing that self-healing hydrogels may lose their properties over time [126,127], but more research is needed in physiological conditions. Also, the effect of *in vivo* conditions, such as enzymes, on these bond's stability needs to be studied as well. [18] In addition to traditional bioink characterization, also the self-healing properties of bioink should be characterized in dept, like Karvinen et al. [51] suggest, i.e., the presence of reversible interactions and their reversibility should be studied, as well as investigating the self-healability of hydrogels and determining the healing efficiencies of hydrogels, not forgetting the time dependence and dynamics of self-healing. In addition, computational modeling in conjunction with sensory-based real-time monitoring systems and closed-loop feedback control algorithms could improve the 3D-bioprinted construct design and quality as they allow optimization of the printing conditions [3].

In general, the future of 3D-bioprinting is moving towards the fabrication of patient-specific, and larger multifunctional tissue/organ grafts, i.e., complex heterocellular tissues with multi-scale vascularization and innervation, and drug delivery systems [7,13,3]. By using a combination of multiple printing techniques, the reduction of the production period and the addition of complexity to architecture and function would be permitted. Functional constructs with heterogeneity, gradients, complexity, and anisotropy could be achieved by using multimaterial 3D-bioprinting. In addition, if, for example, the inclusion of functional nanoparticles within the 3D-bioprinted construct is needed, also the printing technique/instruments could be designed so that an external magnetic, electric, or acoustic field can be applied during the printing, which would help to align, orient, assemble, and distribute the nanoparticles. [7,3]

In 3D-bioprinting, the challenge is that only the initial state of the printed structure is considered and assumed as unchangeable and static, meaning that printed cells would rapidly form, assemble tissues and start synthesizing ECMs, and therefore would provide mechanical properties and maintain the shape. This could be overcome by using 4D-bioprinting. [118,3] In 4D-bioprinting, time is added as the fourth dimension, i.e., the shape or properties of the construct can be changed over time as the tissue forms within the construct [118,52]. The structure can change when exposed to external (e.g., heat, light, moisture, magnetic field, etc.) or intrinsic (e.g., cell forces) stimulus [37,7]. Basically, by using 3D-bioprinting one might mimic native tissue's complex architecture and microenvironment, but using 4D-bioprinting also the dynamic characteristic of complex organs could be achieved [39]. Even though there are no 4D-bioprinting studies using dynamic hydrogels with encapsulated cells, there are already some examples of how, for example, injection is eased by adding a catalyst to dynamic hydrogel, i.e., dynamic properties are modulated at different time points to either allow high injectability or high (long-term) stability for cell culture [128]. However, 4D-bioprinting is not without challenges. For example, cells can affect to the stimuli-responsive materials' responsiveness, or cell viability may be reduced by the material dynamics. In addition, it is also known that in the body, complicated cellular activities are controlled by multiple stimuli, whereas current stimuli-responsive

materials respond to only one stimulus. Thus, 4D-bioprinted constructs that can respond to multiple physiological cues are needed. [27,3] Supramolecular hydrogels would actually be potential candidates as bioink for 4D-bioprinting due to their reversible crosslinks and stimuli-responsive nature [2,12,4,3]. To be noted, Taylor et al. [17] have collected a table of possibly 4D-printable self-healing hydrogels based on their formation method (crosslinking type and gelation time), injectability, self-healing ability, and suitability for reactive printing [17].

5. Conclusions

Self-healing hydrogels have become the most promising ink materials for 3D-bioprinting because unlike traditional hydrogels, the bonds as well as their initial structure, functionality, and properties can be recovered after damage (i.e., extrusion), that together with shear-thinning property, enable safe printing of cells and shape stability of the construct after printing. In addition to their tunable viscoelastic properties, they can also respond to cell forces by rearranging the network, while maintaining bulk physiological properties. The challenges of current self-healing hydrogel inks are, however, how to make printable ink with time-dependent and robust printing performances, i.e., ink with fast recovery time, shear-thinning properties, and suitable yield stress is desired, but even more challenging is how to find ink formulation that is both self-healing and mechanically robust since those properties are usually opposing. Therefore more studies are needed in the future to improve the self-healing hydrogel inks. Currently, as this review shows, mainly extrusion-based bioprinting has been used for dynamic covalent and supramolecular hydrogel inks, couple studies also using inkjet-based bioprinting and stereolithography. With these techniques and crosslinking types used, different 3D-structures (letters, grids, patterns, ears, etc.) have been able to print with high print fidelity. By introducing gel-in-gel printing, more complex spiral, pyramidal, or vascular tree structures have been printed, but even self-standing and overhanging geometries have also been printed without the need of additional support bath. Additionally, by using secondary crosslinking, the stability of the printed constructs have been able to improve. The cell viability has also been high with the aforementioned inks due to the reasons mentioned at the beginning. In general, the future of bioprinting is going towards multimaterial bioprinting, and multifunctional tissue/organ grafts with vascularization and innervation. 4D-bioprinting, in which self-healing hydrogel-based bioinks are very promising, would also provide the needed biomimicking dynamic nature for the construct.

Declaration of Competing Interest

The authors declare that they have no known competing financial interests or personal relationships that could have appeared to influence the work reported in this paper.

Data availability

No data was used for the research described in the article.

Acknowledgements

This work is supported by Academy of Finland (Center of Excellence in Body-on-Chip Research, CoEBoC decision number: 336663 (1.5.2020–31.12.2022) and 353173 (1.1.2023–31.5.2025)). The authors would like to thank Mimosa Peltokangas for conducting thorough background work in her bachelor's thesis for the subject.

References

[1] S. Kyle, Z.M. Jessop, A. Al-Sabah, I.S. Whitaker, 'printability' of candidate biomaterials for extrusion based 3D printing: State-of-the-art, Adv. Healthcare Mater. 6 (16) (2017) 1700264.
[2] S. Ji, M. Guvendiren, Recent advances in bioink design for 3D bioprinting of tissues and organs, Frontiers in bioengineering and biotechnology 5 (2017) 23.
[3] J. Karvinen, M. Kellomäki, Design aspects and characterization of hydrogel-based bioinks for extrusion-based bioprinting, Bioprinting (2023) e00274.
[4] T. Jungst, W. Smolan, K. Schacht, T. Scheibel, J. Groll, Strategies and molecular design criteria for 3D printable hydrogels, Chemical reviews 116 (3) (2016) 1496–1539.
[5] S. Uman, A. Dhand, J.A. Burdick, Recent advances in shear-thinning and self-healing hydrogels for biomedical applications, J. Appl. Polym. Sci. 137 (25) (2020) 48668.
[6] Ž.P. Kačarević, P.M. Rider, S. Alkildani, S. Retnasingh, R. Smeets, O. Jung, Z. Ivanišević, M. Barbeck, An introduction to 3D bioprinting: Possibilities, challenges and future aspects, Materials 11 (11) (2018) 2199.
[7] J. Li, C. Wu, P.K. Chu, M. Gelinsky, 3D printing of hydrogels: Rational design strategies and emerging biomedical applications, Materials Science and Engineering: R: Reports 140 (2020) 100543.
[8] I. Donderwinkel, J.C. Van Hest, N.R. Cameron, Bio-inks for 3D bioprinting: recent advances and future prospects, Polymer Chemistry 8 (31) (2017) 4451–4471.
[9] S.V. Murphy, A. Atala, 3D bioprinting of tissues and organs, Nature biotechnology 32 (8) (2014) 773–785.
[10] P. Heidarian, A.Z. Kouzani, A. Kaynak, M. Paulino, B. Nasri-Nasrabadi, Dynamic hydrogels and polymers as inks for three-dimensional printing, ACS Biomaterials Science & Engineering 5 (6) (2019) 2688–2707.
[11] I. Ozbolat, H. Gudapati, A review on design for bioprinting, Bioprinting 3 (2016) 1–14.
[12] J. Gopinathan, I. Noh, Recent trends in bioinks for 3D printing, Biomaterials research 22 (1) (2018) 11.
[13] A.N. Leberfinger, S. Dinda, Y. Wu, S.V. Koduru, V. Ozbolat, D.J. Ravnic, I. T. Ozbolat, Bioprinting functional tissues, Acta Biomater. 95 (2019) 32–49.
[14] L. Shi, P. Ding, Y. Wang, Y. Zhang, D. Ossipov, J. Hilborn, Self-healing polymeric hydrogel formed by metal–ligand coordination assembly: Design, fabrication, and biomedical applications, Macromolecular rapid communications 40 (7) (2019) 1800837.
[15] S. Hafeez, H.W. Ooi, F.L. Morgan, C. Mota, M. Dettin, C. Van Blitterswijk, L. Moroni, M.B. Baker, Viscoelastic oxidized alginates with reversible imine type crosslinks: self-healing, injectable, and bioprintable hydrogels, Gels 4 (4) (2018) 85.
[16] Y. Tu, N. Chen, C. Li, H. Liu, R. Zhu, S. Chen, Q. Xiao, J. Liu, S. Ramakrishna, L. He, Advances in injectable self-healing biomedical hydrogels, Acta Biomater. 90 (2019) 1–20.
[17] D.L. Taylor, M. in het Panhuis, Self-healing hydrogels, Adv. Mater. 28 (41) (2016) 9060–9093.
[18] A. Devi VK, R. Shyam, A. Palaniappan, A.K. Jaiswal, T.-H. Oh, A.J. Nathanael, Self-healing hydrogels: Preparation, mechanism and advancement in biomedical applications, Polymers 13 (21) (2021) 3782.
[19] B. Gyarmati, B.A. Szilágyi, A. Szilágyi, Reversible interactions in self-healing and shape memory hydrogels, Eur. Polymer J. 93 (2017) 642–669.
[20] Z. Deng, H. Wang, P.X. Ma, B. Guo, Self-healing conductive hydrogels: preparation, properties and applications, Nanoscale 12 (3) (2020) 1224–1246.
[21] M.H. Chen, L.L. Wang, J.J. Chung, Y.-H. Kim, P. Atluri, J.A. Burdick, Methods to assess shear-thinning hydrogels for application as injectable biomaterials, ACS biomaterials science & engineering 3 (12) (2017) 3146–3160.
[22] M. Hafezi, S.N. Khorasani, S. Khalili, R.E. Neisiany, Self-healing interpenetrating network hydrogel based on gelma/alginate/nano-clay, Int. J. Biol. Macromol. 242 (2023) 124962.
[23] O. Jeon, Y.B. Lee, S.J. Lee, N. Guliyeva, J. Lee, E. Alsberg, Stem cell-laden hydrogel bioink for generation of high resolution and fidelity engineered tissues with complex geometries, Bioactive materials 15 (2022) 185–193.
[24] S. Talebian, M. Mehrali, N. Taebnia, C.P. Pennisi, F.B. Kadumudi, J. Foroughi, M. Hasany, M. Nikkhah, M. Akbari, G. Orive, et al., Self-healing hydrogels: the next paradigm shift in tissue engineering? Advanced Science 6 (16) (2019) 1801664.
[25] X. Ding, L. Fan, L. Wang, M. Zhou, Y. Wang, Y. Zhao, Designing self-healing hydrogels for biomedical applications, Materials Horizons.
[26] G.T. Jacob, V.E. Passamai, S. Katz, G.R. Castro, V. Alvarez, Hydrogels for extrusion-based bioprinting: General considerations, Bioprinting 27 (2022) e00212.
[27] J.M. Unagolla, A.C. Jayasuriya, Hydrogel-based 3D bioprinting: A comprehensive review on cell-laden hydrogels, bioink formulations, and future perspectives, Applied Materials Today 18 (2020) 100479.
[28] K. Hölzl, S. Lin, L. Tytgat, S. Van Vlierberghe, L. Gu, A. Ovsianikov, Bioink properties before, during and after 3D bioprinting, Biofabrication 8 (3) (2016) 032002.
[29] S.A. Irvine, S.S. Venkatraman, Bioprinting and differentiation of stem cells, Molecules 21 (9) (2016) 1188.
[30] J.M. Lee, W.Y. Yeong, Design and printing strategies in 3D bioprinting of cell-hydrogels: A review, Adv. Healthcare Mater. 5 (22) (2016) 2856–2865.
[31] Y. Wu, Y. Zhang, M. Yan, G. Hu, Z. Li, W. He, X. Wang, A. Abulimit, R. Li, Research progress on the application of inkjet printing technology combined with hydrogels, Applied Materials Today 36 (2024) 102036.

[32] A. Zennifer, A. Subramanian, S. Sethuraman, Design considerations of bioinks for laser bioprinting technique towards tissue regenerative applications, Bioprinting 27 (2022) e00205.
[33] W. Li, M. Wang, H. Ma, F.A. Chapa-Villarreal, A.O. Lobo, Y.S. Zhang, Stereolithography apparatus and digital light processing-based 3d bioprinting for tissue fabrication, Iscience 26 (2023) 106039.
[34] C. Li, A. Faulkner-Jones, A.R. Dun, J. Jin, P. Chen, Y. Xing, Z. Yang, Z. Li, W. Shu, D. Liu, et al., Rapid formation of a supramolecular polypeptide–DNA hydrogel for in situ three-dimensional multilayer bioprinting, Angew. Chem. 127 (13) (2015) 4029–4033.
[35] H. Chen, B. Hao, P. Ge, S. Chen, Highly stretchable, self-healing, and 3D printing prefabricatable hydrophobic association hydrogels with the assistance of electrostatic interaction, Polymer Chemistry 11 (29) (2020) 4741–4748.
[36] C.B. Highley, K.H. Song, A.C. Daly, J.A. Burdick, Jammed microgel inks for 3D printing applications, Advanced Science 6 (1) (2019) 1801076.
[37] K.A. Deo, K.A. Singh, C.W. Peak, D.L. Alge, A.K. Gaharwar, Bioprinting 101: design, fabrication, and evaluation of cell-laden 3D bioprinted scaffolds, Tissue Eng. Part A 26 (5–6) (2020) 318–338.
[38] A. Schwab, R. Levato, M. D'Este, S. Piluso, D. Eglin, J. Malda, Printability and shape fidelity of bioinks in 3D bioprinting, Chemical reviews 120 (19) (2020) 11028–11055.
[39] P. Dorishetty, N.K. Dutta, N.R. Choudhury, Bioprintable tough hydrogels for tissue engineering applications, Adv. Colloid Interface Sci. (2020) 102163.
[40] A. Panwar, L.P. Tan, Current status of bioinks for micro-extrusion-based 3D bioprinting, Molecules 21 (6) (2016) 685.
[41] H. Li, C. Tan, L. Li, Review of 3D printable hydrogels and constructs, Materials & Design 159 (2018) 20–38.
[42] J.M. Townsend, E.C. Beck, S.H. Gehrke, C.J. Berkland, M.S. Detamore, Flow behavior prior to crosslinking: The need for precursor rheology for placement of hydrogels in medical applications and for 3D bioprinting, Prog. Polym. Sci. 91 (2019) 126–140.
[43] U. Jammalamadaka, K. Tappa, Recent advances in biomaterials for 3D printing and tissue engineering, Journal of functional biomaterials 9 (1) (2018) 22.
[44] Y. Liu, C.-W. Wong, S.-W. Chang, S.-H. Hsu, An injectable, self-healing phenol-functionalized chitosan hydrogel with fast gelling property and visible light-crosslinking capability for 3D printing, Acta Biomater. 122 (2021) 211–219.
[45] M.E. Cooke, D.H. Rosenzweig, The rheology of direct and suspended extrusion bioprinting, APL bioengineering 5 (1) (2021) 011502.
[46] S. Seiffert, E. Kumacheva, O. Okay, M. Anthamatten, M. Chau, P.Y. Dankers, B. W. Greenland, W. Hayes, P. Li, R. Liu, et al., Supramolecular polymer networks and gels, Vol. 268, Springer, 2015.
[47] C.B. Highley, C.B. Rodell, J.A. Burdick, Direct 3D printing of shear-thinning hydrogels into self-healing hydrogels, Adv. Mater. 27 (34) (2015) 5075–5079.
[48] Y.S. Zhang, K. Yue, J. Aleman, K. Mollazadeh-Moghaddam, S.M. Bakht, J. Yang, W. Jia, V. Dell'Erba, P. Assawes, S.R. Shin, et al., 3D bioprinting for tissue and organ fabrication, Annals of biomedical engineering 45 (1) (2017) 148–163.
[49] K.H. Song, C.B. Highley, A. Rouff, J.A. Burdick, Complex 3d-printed microchannels within cell-degradable hydrogels, Adv. Funct. Mater. 28 (31) (2018) 1801331.
[50] C. Xu, G. Dai, Y. Hong, Recent advances in high-strength and elastic hydrogels for 3D printing in biomedical applications, Acta Biomater. 95 (2019) 50–59.
[51] J. Karvinen, M. Kellomäki, Characterization of self-healing hydrogels for biomedical applications, Eur. Polymer J. 181 (2022) 111641.
[52] F.L. Morgan, L. Moroni, M.B. Baker, Dynamic bioinks to advance bioprinting, Adv. Healthcare Mater. 9 (15) (2020) 1901798.
[53] Z. Tong, L. Jin, J.M. Oliveira, R.L. Reis, Q. Zhong, Z. Mao, C. Gao, Adaptable hydrogel with reversible linkages for regenerative medicine: Dynamic mechanical microenvironment for cells, Bioactive materials 6 (5) (2021) 1375–1387.
[54] C.M. Madl, S.C. Heilshorn, Engineering hydrogel microenvironments to recapitulate the stem cell niche, Annual review of biomedical engineering 20 (2018) 21–47.
[55] C. Argentati, F. Morena, I. Tortorella, M. Bazzucchi, S. Porcellati, C. Emiliani, S. Martino, Insight into mechanobiology: how stem cells feel mechanical forces and orchestrate biological functions, International journal of molecular sciences 20 (21) (2019) 5337.
[56] I. Levental, P.C. Georges, P.A. Janmey, Soft biological materials and their impact on cell function, Soft Matter 3 (3) (2007) 299–306.
[57] A.R. Cameron, J.E. Frith, J.J. Cooper-White, The influence of substrate creep on mesenchymal stem cell behaviour and phenotype, Biomaterials 32 (26) (2011) 5979–5993.
[58] O. Chaudhuri, L. Gu, D. Klumpers, M. Darnell, S.A. Bencherif, J.C. Weaver, N. Huebsch, H.-P. Lee, E. Lippens, G.N. Duda, et al., Hydrogels with tunable stress relaxation regulate stem cell fate and activity, Nat. Mater. 15 (3) (2016) 326–334.
[59] T.-C. Tseng, L. Tao, F.-Y. Hsieh, Y. Wei, I.-M. Chiu, S.-H. Hsu, An injectable, self-healing hydrogel to repair the central nervous system, Adv. Mater. 27 (23) (2015) 3518–3524.
[60] K. Brännvall, K. Bergman, U. Wallenquist, S. Svahn, T. Bowden, J. Hilborn, K. Forsberg-Nilsson, Enhanced neuronal differentiation in a three-dimensional collagen-hyaluronan matrix, Journal of neuroscience research 85 (10) (2007) 2138–2146.
[61] S.K. Seidlits, Z.Z. Khaing, R.R. Petersen, J.D. Nickels, J.E. Vanscoy, J.B. Shear, C. E. Schmidt, The effects of hyaluronic acid hydrogels with tunable mechanical properties on neural progenitor cell differentiation, Biomaterials 31 (14) (2010) 3930–3940.
[62] N.D. Leipzig, M.S. Shoichet, The effect of substrate stiffness on adult neural stem cell behavior, Biomaterials 30 (36) (2009) 6867–6878.
[63] K. Uto, J.H. Tsui, C.A. DeForest, D.-H. Kim, Dynamically tunable cell culture platforms for tissue engineering and mechanobiology, Progress in polymer science 65 (2017) 53–82.
[64] S. Nam, J. Lee, D.G. Brownfield, O. Chaudhuri, Viscoplasticity enables mechanical remodeling of matrix by cells, Biophysical journal 111 (10) (2016) 2296–2308.
[65] D.D. McKinnon, D.W. Domaille, J.N. Cha, K.S. Anseth, Biophysically defined and cytocompatible covalently adaptable networks as viscoelastic 3D cell culture systems, Adv. Mater. 26 (6) (2014) 865–872.
[66] W. Zhang, K. Zhang, S. Yan, J. Wu, J. Yin, A tough and self-healing poly (L-glutamic acid)-based composite hydrogel for tissue engineering, J. Mater. Chem. B 6 (42) (2018) 6865–6876.
[67] H. Wang, D. Zhu, A. Paul, L. Cai, A. Enejder, F. Yang, S.C. Heilshorn, Covalently adaptable elastin-like protein–hyaluronic acid (ELP–HA) hybrid hydrogels with secondary thermoresponsive crosslinking for injectable stem cell delivery, Advanced functional materials 27 (28) (2017) 1605609.
[68] X. Zhao, N. Huebsch, D.J. Mooney, Z. Suo, Stress-relaxation behavior in gels with ionic and covalent crosslinks, Journal of applied physics 107 (6) (2010) 063509.
[69] X. Li, Q. Sun, Q. Li, N. Kawazoe, G. Chen, Functional hydrogels with tunable structures and properties for tissue engineering applications, Frontiers in chemistry 6 (2018) 499.
[70] J. Lou, R. Stowers, S. Nam, Y. Xia, O. Chaudhuri, Stress relaxing hyaluronic acid-collagen hydrogels promote cell spreading, fiber remodeling, and focal adhesion formation in 3d cell culture, Biomaterials 154 (2018) 213–222.
[71] H.-P. Lee, L. Gu, D.J. Mooney, M.E. Levenston, O. Chaudhuri, Mechanical confinement regulates cartilage matrix formation by chondrocytes, Nat. Mater. 16 (12) (2017) 1243–1251.
[72] S.W. Crowder, V. Leonardo, T. Whittaker, P. Papathanasiou, M.M. Stevens, Material cues as potent regulators of epigenetics and stem cell function, Cell stem cell 18 (1) (2016) 39–52.
[73] S. Tang, H. Ma, H.-C. Tu, H.-R. Wang, P.-C. Lin, K.S. Anseth, Adaptable fast relaxing boronate-based hydrogels for probing cell–matrix interactions, Advanced Science 5 (9) (2018) 1800638.
[74] J. Malda, J. Visser, F.P. Melchels, T. Jüngst, W.E. Hennink, W.J. Dhert, J. Groll, D. W. Hutmacher, 25th anniversary article: engineering hydrogels for biofabrication, Adv. Mater. 25 (36) (2013) 5011–5028.
[75] A. Abbadessa, M. Blokzijl, V. Mouser, P. Marica, J. Malda, W. Hennink, T. Vermonden, A thermo-responsive and photo-polymerizable chondroitin sulfate-based hydrogel for 3d printing applications, Carbohydrate polymers 149 (2016) 163–174.
[76] S.M. Hull, L.G. Brunel, S.C. Heilshorn, 3d bioprinting of cell-laden hydrogels for improved biological functionality, Adv. Mater. 34 (2) (2022) 2103691.
[77] K. Dubbin, A. Tabet, S.C. Heilshorn, Quantitative criteria to benchmark new and existing bio-inks for cell compatibility, Biofabrication 9 (4) (2017) 044102.
[78] L. Cai, R.E. Dewi, A.B. Goldstone, J.E. Cohen, A.N. Steele, Y.J. Woo, S. C. Heilshorn, Regulating stem cell secretome using injectable hydrogels with in situ network formation, Adv. Healthcare Mater. 5 (21) (2016) 2758–2764.
[79] C.W. Peak, J. Stein, K.A. Gold, A.K. Gaharwar, Nanoengineered colloidal inks for 3D bioprinting, Langmuir 34 (3) (2018) 917–925.
[80] F.-Y. Hsieh, L. Tao, Y. Wei, S.-H. Hsu, A novel biodegradable self-healing hydrogel to induce blood capillary formation, Npg Asia Materials 9 (3) (2017) e363–e363.
[81] Y. Wang, X. Huang, Y. Shen, R. Hang, X. Zhang, Y. Wang, X. Yao, B. Tang, Direct writing alginate bioink inside pre-polymers of hydrogels to create patterned vascular networks, J. Mater. Sci. 54 (2019) 7883–7892.
[82] Y. Fang, Y. Guo, B. Wu, Z. Liu, M. Ye, Y. Xu, M. Ji, L. Chen, B. Lu, K. Nie, et al., Expanding embedded 3D bioprinting capability for engineering complex organs with freeform vascular networks, Adv. Mater. (2023) 2205082.
[83] S. Das, W.J. Gordián-Vélez, H.C. Ledebur, F. Mourkioti, P. Rompolas, H.I. Chen, M.D. Serruya, D.K. Cullen, Innervation: the missing link for biofabricated tissues and organs, NPJ Regenerative medicine 5 (1) (2020) 11.
[84] A. Marrella, T.Y. Lee, D.H. Lee, S. Karuthedom, D. Syla, A. Chawla, A. Khademhosseini, H.L. Jang, Engineering vascularized and innervated bone biomaterials for improved skeletal tissue regeneration, Mater. Today 21 (4) (2018) 362–376.
[85] H. Oliveira, C. Médina, M.-L. Stachowicz, B.P. dos Santos, L. Chagot, N. Dusserre, J.-C. Fricain, Extracellular matrix (ecm)-derived bioinks designed to foster vasculogenesis and neurite outgrowth: Characterization and bioprinting, Bioprinting 22 (2021) e00134.
[86] N. Diamantides, C. Dugopolski, E. Blahut, S. Kennedy, L.J. Bonassar, High density cell seeding affects the rheology and printability of collagen bioinks, Biofabrication 11 (4) (2019) 045016.
[87] T. Billiet, E. Gevaert, T. De Schryver, M. Cornelissen, P. Dubruel, The 3D printing of gelatin methacrylamide cell-laden tissue-engineered constructs with high cell viability, Biomaterials 35 (1) (2014) 49–62.
[88] B.G. Maisonneuve, D.C. Roux, P. Thorn, J.J. Cooper-White, Effects of cell density and biomacromolecule addition on the flow behavior of concentrated mesenchymal cell suspensions, Biomacromolecules 14 (12) (2013) 4388–4397.
[89] J. Cheng, F. Lin, H. Liu, Y. Yan, X. Wang, R. Zhang, Z. Xiong, Rheological properties of cell-hydrogel composites extruding through small-diameter tips, Journal of manufacturing science and engineering 130 (2).
[90] N. Majumder, A. Mishra, S. Ghosh, Effect of varying cell densities on the rheological properties of the bioink, Bioprinting 28 (2022) e00241.
[91] A. Skardal, J. Zhang, L. McCoard, S. Oottamasathien, G.D. Prestwich, Dynamically crosslinked gold nanoparticle–hyaluronan hydrogels, Adv. Mater. 22 (42) (2010) 4736–4740.

[92] L.L. Wang, C.B. Highley, Y.-C. Yeh, J.H. Galarraga, S. Uman, J.A. Burdick, Three-dimensional extrusion bioprinting of single-and double-network hydrogels containing dynamic covalent crosslinks, Journal of Biomedical Materials Research Part A 106 (4) (2018) 865–875.
[93] Q. Liu, N. Ji, L. Xiong, Q. Sun, Rapid gelling, self-healing, and fluorescence-responsive chitosan hydrogels formed by dynamic covalent crosslinking, Carbohydr. Polym. 246 (2020) 116586.
[94] H. Chen, F. Fei, X. Li, Z. Nie, D. Zhou, L. Liu, J. Zhang, H. Zhang, Z. Fei, T. Xu, A structure-supporting, self-healing, and high permeating hydrogel bioink for establishment of diverse homogeneous tissue-like constructs, Bioactive materials 6 (10) (2021) 3580–3595.
[95] E.S. Ko, C. Kim, Y. Choi, K.Y. Lee, 3D printing of self-healing ferrogel prepared from glycol chitosan, oxidized hyaluronate, and iron oxide nanoparticles, Carbohydr. Polym. 245 (2020) 116496.
[96] Y. Choi, C. Kim, H.S. Kim, C. Moon, K.Y. Lee, 3D printing of dynamic tissue scaffold by combining self-healing hydrogel and self-healing ferrogel, Colloids Surf., B 208 (2021) 112108.
[97] S.W. Kim, D.Y. Kim, H.H. Roh, H.S. Kim, J.W. Lee, K.Y. Lee, Three-dimensional bioprinting of cell-laden constructs using polysaccharide-based self-healing hydrogels, Biomacromolecules 20 (5) (2019) 1860–1866.
[98] H.-H. Roh, H.-S. Kim, C. Kim, K.-Y. Lee, 3D printing of polysaccharide-based self-healing hydrogel reinforced with alginate for secondary cross-linking, Biomedicines 9 (9) (2021) 1224.
[99] W. Zhang, M. Kuss, Y. Yan, W. Shi, Dynamic alginate hydrogel as an antioxidative bioink for bioprinting, Gels 9 (4) (2023) 312.
[100] C. Loebel, C.B. Rodell, M.H. Chen, J.A. Burdick, Shear-thinning and self-healing hydrogels as injectable therapeutics and for 3D-printing, Nature protocols 12 (8) (2017) 1521.
[101] L. Ouyang, R. Yao, Y. Zhao, W. Sun, Effect of bioink properties on printability and cell viability for 3D bioplotting of embryonic stem cells, Biofabrication 8 (3) (2016) 035020.
[102] Z. Wang, G. An, Y. Zhu, X. Liu, Y. Chen, H. Wu, Y. Wang, X. Shi, C. Mao, 3D-printable self-healing and mechanically reinforced hydrogels with host–guest non-covalent interactions integrated into covalently linked networks, Materials horizons 6 (4) (2019) 733–742.
[103] L. Shi, H. Carstensen, K. Hölzl, M. Lunzer, H. Li, J. Hilborn, A. Ovsianikov, D. A. Ossipov, Dynamic coordination chemistry enables free directional printing of biopolymer hydrogel, Chem. Mater. 29 (14) (2017) 5816–5823.
[104] B.A. de Melo, Y.A. Jodat, S. Mehrotra, M.A. Calabrese, T. Kamperman, B. B. Mandal, M.H. Santana, E. Alsberg, J. Leijten, S.R. Shin, 3D printed cartilage-like tissue constructs with spatially controlled mechanical properties, Advanced functional materials 29 (51) (2019) 1906330.
[105] C.D. Lindsay, J.G. Roth, B.L. LeSavage, S.C. Heilshorn, Bioprinting of stem cell expansion lattices, Acta biomaterialia 95 (2019) 225–235.
[106] S. Song, Y. Li, J. Huang, S. Cheng, Z. Zhang, Inhibited astrocytic differentiation in neural stem cell-laden 3D bioprinted conductive composite hydrogel scaffolds for repair of spinal cord injury, Biomaterials Advances 148 (2023) 213385.
[107] K. Dubbin, Y. Hori, K.K. Lewis, S.C. Heilshorn, Dual-stage crosslinking of a gel-phase bioink improves cell viability and homogeneity for 3D bioprinting, Adv. Healthcare Mater. 5 (19) (2016) 2488–2492.
[108] M. Zhang, A. Vora, W. Han, R.J. Wojtecki, H. Maune, A.B. Le, L.E. Thompson, G. M. McClelland, F. Ribet, A.C. Engler, et al., Dual-responsive hydrogels for direct-write 3D printing, Macromolecules 48 (18) (2015) 6482–6488.
[109] N. Sällström, A. Capel, M.P. Lewis, D.S. Engstrøm, S. Martin, 3d-printable zwitterionic nano-composite hydrogel system for biomedical applications, Journal of Tissue Engineering 11 (2020), 2041731420967294.
[110] N. Sällström, A. Goulas, S. Martin, D.S. Engstrøm, The effect of print speed and material aging on the mechanical properties of a self-healing nanocomposite hydrogel, Additive Manufacturing 35 (2020) 101253.
[111] S. Maiz-Fernández, N. Barroso, L. Pérez-Álvarez, U. Silván, J.L. Vilas-Vilela, S. Lanceros-Mendez, 3D printable self-healing hyaluronic acid/chitosan polycomplex hydrogels with drug release capability, Int. J. Biol. Macromol. 188 (2021) 820–832.
[112] Y.S. Zhang, R. Oklu, M.R. Dokmeci, A. Khademhosseini, Three-dimensional bioprinting strategies for tissue engineering, Cold Spring Harbor perspectives in medicine 8 (2) (2018) a025718.
[113] A. Blaeser, D.F. Duarte Campos, U. Puster, W. Richtering, M.M. Stevens, H. Fischer, Controlling shear stress in 3D bioprinting is a key factor to balance printing resolution and stem cell integrity, Adv. Healthcare Mater. 5 (3) (2016) 326–333.
[114] C. Loebel, R.L. Mauck, J.A. Burdick, Local nascent protein deposition and remodelling guide mesenchymal stromal cell mechanosensing and fate in three-dimensional hydrogels, Nat. Mater. 18 (8) (2019) 883–891.
[115] L. Zou, A.S. Braegelman, M.J. Webber, Dynamic supramolecular hydrogels spanning an unprecedented range of host–guest affinity, ACS applied materials & interfaces 11 (6) (2019) 5695–5700.
[116] J.-Y. Sun, X. Zhao, W.R. Illeperuma, O. Chaudhuri, K.H. Oh, D.J. Mooney, J. J. Vlassak, Z. Suo, Highly stretchable and tough hydrogels, Nature 489 (7414) (2012) 133–136.
[117] T.L. Sun, T. Kurokawa, S. Kuroda, A.B. Ihsan, T. Akasaki, K. Sato, M.A. Haque, T. Nakajima, J.P. Gong, Physical hydrogels composed of polyampholytes demonstrate high toughness and viscoelasticity, Nat. Mater. 12 (10) (2013) 932–937.
[118] B. Gao, Q. Yang, X. Zhao, G. Jin, Y. Ma, F. Xu, 4D bioprinting for biomedical applications, Trends Biotechnol. 34 (9) (2016) 746–756.
[119] P. Heidarian, A.Z. Kouzani, A self-healing nanocomposite double network bacterial nanocellulose/gelatin hydrogel for three dimensional printing, Carbohydr. Polym. (2023) 120879.
[120] F. Dalloul, J.B. Mietner, J.R. Navarro, Three-dimensional printing of a tough polymer composite gel ink reinforced with chemically modified cellulose nanofibrils showing self-healing behavior, ACS Appl. Polymer Mater.
[121] H. Zhu, M. Monavari, K. Zheng, T. Distler, L. Ouyang, S. Heid, Z. Jin, J. He, D. Li, A.R. Boccaccini, 3D bioprinting of multifunctional dynamic nanocomposite bioinks incorporating Cu-doped mesoporous bioactive glass nanoparticles for bone tissue engineering, Small 18 (12) (2022) 2104996.
[122] M. Lee, K. Bae, C. Levinson, M. Zenobi-Wong, Nanocomposite bioink exploits dynamic covalent bonds between nanoparticles and polysaccharides for precision bioprinting, Biofabrication 12 (2) (2020) 025025.
[123] B.O. Okesola, A. Mata, Multicomponent self-assembly as a tool to harness new properties from peptides and proteins in material design, Chem. Soc. Rev. 47 (10) (2018) 3721–3736.
[124] B.O. Okesola, Y. Wu, B. Derkus, S. Gani, D. Wu, D. Knani, D.K. Smith, D.J. Adams, A. Mata, Supramolecular self-assembly to control structural and biological properties of multicomponent hydrogels, Chem. Mater. 31 (19) (2019) 7883–7897.
[125] M. Zhang, X. Chen, K. Yang, Q. Dong, H. Yang, S. Gu, W. Xu, Y. Zhou, Dual-crosslinked hyaluronic acid hydrogel with self-healing capacity and enhanced mechanical properties, Carbohydr. Polym. 301 (2023) 120372.
[126] T. Kakuta, Y. Takashima, M. Nakahata, M. Otsubo, H. Yamaguchi, A. Harada, Preorganized hydrogel: self-healing properties of supramolecular hydrogels formed by polymerization of host–guest-monomers that contain cyclodextrins and hydrophobic guest groups, Adv. Mater. 25 (20) (2013) 2849–2853.
[127] H. Zhang, H. Xia, Y. Zhao, Poly (vinyl alcohol) hydrogel can autonomously self-heal, ACS Macro Letters 1 (11) (2012) 1233–1236.
[128] J. Lou, F. Liu, C.D. Lindsay, O. Chaudhuri, S.C. Heilshorn, Y. Xia, Dynamic hyaluronan hydrogels with temporally modulated high injectability and stability using a biocompatible catalyst, Adv. Mater. 30 (22) (2018) 1705215.